DESIGN OF AN OVER-COUPLED COAXIAL RESONATOR FOR DETERMINING THE ELECTRICAL PROPERTIES OF MATERIALS

A Thesis

Submitted to the Faculty of Graduate Studies and Research

In Partial Fulfilment of the Requirements

For the Degree of

Master of Applied Science

in

Electronic Systems Engineering University of Regina

By

Muhammed Bashiru Suleman

Regina, Saskatchewan

September, 2017

UNIVERSITY OF REGINA

FACULTY OF GRADUATE STUDIES AND RESEARCH

SUPERVISORY AND EXAMINING COMMITTEE

Muhammed Bashiru Suleman, candidate for the degree of Master of Applied Science in Electronic Systems Engineering**,** has presented a thesis titled, ***Design of an Over-Coupled Coaxial Resonator for Determining the Electrical Properties of Materials,*** in an oral examination held on August 18, 2017. The following committee members have found the thesis acceptable in form and content, and that the candidate demonstrated satisfactory knowledge of the subject material.

External Examiner:	Dr. Craig Gelowitz, Software Systems Engineering
Supervisor:	Dr. Paul Laforge, Electronic Systems Engineering
Committee Member:	Dr. Irfan Al-Anbagi, Electronic Systems Engineering
Committee Member:	Dr. Shahid Azam, Environmental Systems Engineering
Chair of Defense:	Dr. Gale Russell, Faculty of Education

Abstract

Material characterisation has helped in various engineering purposes, providing useful knowledge so that different materials can be adapted for varying purposes. For example, materials used in engineering design and processes. With unique properties of every material, there is need to determine the properties and characterise materials based on their properties, where their electrical properties is dependent on the dielectric properties of the materials.

In this thesis, a method used in determining the electrical properties of materials using the group delay information is investigated. A gap-coupled coaxial resonator that operates in an over-coupled state is designed and used in obtaining the dielectric properties of sample materials.

Electromagnetic and circuit simulation tools (HFSS and ADS) are used to better understand and develop the concepts used in this study. Simple lumped elements and distributed elements are used in ADS to model coupled resonators so as to arrive at a set of equations to characterise the coupled resonator when it is empty and filled with a dielectric sample. With HFSS, a model of gap-coupled coaxial resonator is designed and analysed. Where the gap provides the capacitance required for coupling electromagnetic field into the resonator. Different known values of dielectric constant are tested and evaluated using the set of equations obtained. The results from the simulations are used to arrive at certain design parameters for fabricating the resonator. With the physical resonator, Teflon is tested to determine its electrical properties. The results from both the simulation and the fabricated resonator show dielectric constant and loss tangent values obtained to be within the known limits of Teflon.

Acknowledgements

First of all, I want to thank my creator for everything, and for seeing me through my program. The success of this work and my academic pursuit has always been through His Grace.

Special thanks to my supervisor, Dr. Paul Laforge for the life changing opportunity to work with him. His guidance, immense directions and support which most especially included financial grants contributed to the success of this research work. Also, I owe the success of this work to the contributions of Chris Yung from Engineering Workshop. His professional services were exceptional.

Additionally, I want to acknowledge Faculty of graduate studies, Department of Electronic System Engineering for the scholarships and teaching assistantship positions I received.

To my mom, I want to thank her for her love and prayers. Appreciation also goes to my friends and family members for their understanding and support as well as Mrs. Alice Williams for her care during my stay in Regina.

Table of Contents

List of Figures

List of Tables

Abbreviations & Notations

ADS - Advanced Design System

HFSS- High Frequency Electromagnetic Field Simulation

RLC-Resistor Inductor Capacitor

VNA- Vector Network Analyser

$\boldsymbol{\varepsilon_r}$ – Relative Dielectric Permittivity

$\boldsymbol{\varepsilon_o}$ – Absolute Permittivity of Free Space (8.85×10^{-12} (F/m))

$\boldsymbol{\varepsilon}$ - Dielectric Permittivity

$\boldsymbol{S_{11}}$ – Input Reflection Coefficient

$\boldsymbol{\gamma_t}$ – Propagation Constant

$\boldsymbol{\beta}$ – Phase Constant

$\boldsymbol{\alpha}$ – Attenuation Constant

$\Gamma_{\boldsymbol{d}}$ – Group Delay of the Input Reflection Coefficient

$\boldsymbol{\varphi}$ – Phase

$\boldsymbol{\mu_o}$ – Absolute Permeability ($4\pi \times 10^{-7} \mathrm{H \cdot m^{-1}}$)

$\boldsymbol{\mu}$ – Permeability

$\boldsymbol{\omega}$ – Angular Frequency

$\boldsymbol{\omega_o}$ – Angular Resonant frequency

$\boldsymbol{c}$ - Speed of Light (3×10^8 m/s)

$\boldsymbol{\lambda_o}$- Wavelength of free space

$\boldsymbol{\lambda_c}$- Cut- off wavelength

Chapter 1 **: Introduction**

1.1 Introduction

Materials (matter) can be generally characterised based on the degree of electrical conduction as: conductors of electricity and non-conductors of electricity. In reality, 'non-conducting' materials are better termed as poor conductors because they actually conduct electric current to a certain degree, this class of materials can be best described by the dielectric properties of the materials. The behaviour of electromagnetic fields on interaction with the material could be a suitable means of sensing other properties of the material (Nelson, 2010), which can be correlated to the dielectric properties (if they are poor conductors). This identified electrical behaviour of a given material can be used to predict and/or understand other properties of the material which may not be limited to physical and chemical properties of the material being studied as well as adapting it for other applications like engineering designs and/or manufacturing processes.

Significant progress has been made in material characterisation with different methods and techniques that suit each kind of material operating in certain conditions. For soil characterisation studies for example, its usefulness cannot be over-emphasised because soil itself is useful to man (we build structures and they also play a paramount role in agriculture). Different soil types require separate treatments as regards to what exactly it is being applied for. For contaminated soils, the ability to remove the contaminations can be safely done if the original properties of the natural soil are well known as the contaminations tend to alter the properties of the resultant soil.

The responses on applying electromagnetic fields to any given material, such as a soil sample or any given material, gives some interesting results (depending on the methods

and/or conditions) which can to a large extent help to describe the characteristics of the material in terms of its ability to store energy or the losses associated with the application of the electric fields. The conditions that affect material characterisation can be: its original constituents that make up the material, the temperature at which test is done, density, frequency etc. These tend to vary the results of measurement when the same sample is subjected to test under different conditions. However, some materials like Teflon, show fairly constant measurements when the tests are done over a range of frequencies and other conditions.

1.2 Research Objectives

The main objective of this study is to design an over-coupled coaxial resonator measuring device that can be used in obtaining dielectric values of sample materials.

The specific objectives are as follows:

- To model an over-coupled coaxial resonator using the phase information of the reflected input signal.
- To design a gap-coupled coaxial resonator measuring device.
- To evaluate the electrical properties of known materials using the reflected group delay information of electromagnetic signal.

1.3 Contributions

The main contributions of this thesis are:

- Developing a procedure to use the reflected group delay of an over-coupled resonator to determine the dielectric properties of a material.

- Designing, fabricating and testing an over-coupled resonator and using it to determine the dielectric properties material of Teflon.
- Advancing the knowledge of the reflected group delay method for designing lossy filters.

1.4 Thesis Outline

With the introduction in chapter 1, chapter 2 contains a review of literature; the theory of a material sample like soil is considered. An overview of dielectric subject matter and methods of determining the dielectric properties of a material. Transmission line theory as well as background information on the concept of reflected group delay were discussed.

To understand the approach to the research work, chapter 3 presents microwave analysis of coupled resonators (lumped element model and distributed circuits) detailing mathematical concepts and simulations that help to describe both lumped element models and distributed circuit analysis of lossless and lossy resonators. This model analysis basically acts as a precursor to the group delay approach used in studying a lossless and lossy resonator (when it is empty and when it contains a dielectric sample).

Chapter 4 discusses the proposed model for the over-coupled coaxial resonator measuring device with simulations used to evaluate the dielectric permittivity of a sample and quality factor of the resonator to validate the proposed method. Chapter 5 discusses the experiment/tests performed using the fabricated design model using samples of known permittivity values and conclusions are presented in chapter 6.

Chapter 2 **: Literature Review**

2.1 Introduction

Since the main driver of this work is to determine the electrical properties of soils, this chapter begins with the review of the theory of soil, highlighting the characteristics of a two-phase system of soil containing water. Soil composition is used in the classification of various soil samples as it relates to mineral particles. Next, theoretical background on electromagnetic propagation in a medium is established. This includes various techniques used to determine the electrical properties of the materials (dielectric permittivity, quality factor, loss tangent etc). Their basic concepts are studied in relation to the frequency of propagation used to characterise a material's electrical properties.

2.2 Soil-Water System

The accumulation of mineral particles formed by the weathering of rocks can be termed soil. These weathered rocks have void spaces between them which contain water and/or air. When it contains water only it is referred to as a soil-water system (a two-phase soil system). The presence of water in soil greatly changes the behaviour of soil. This was affirmed by Karl Terzaghi (Palanikumar, 2013) who concluded that in engineering practice, the challenges observed in soil are not only due to soil itself but the water contained in the void**.** For this reason water present in soil plays a role in its properties, therefore, knowledge of the soil structure is important. This will provide a better understanding of the soil mineralogy, particles-water interface interaction as well as arrangement of particles of soil. This can be useful in evaluating contamination migration in soil, soil swelling potential, erosion potential etc. (Arulanandan, 2003).

2.2.1 Soil Composition

Soil is composed of particles (solid, liquid & gas) that vary in sizes and shapes (spherical, bulky grains to thin, flat plates and long, slender needles). Soil minerals contain mostly elements found in earth crust e.g. oxygen, hydrogen, silicon, aluminium, sodium, potassium. The mineralogical composition determines the size, shape and surface characteristics of soil particles as well as influencing the interaction of soil in its fluid phase. Using the sizes of soil particles, soil can be classified into sand, silt and clay. The particle size limits associated with the classification are given below:

Table 2.1 Sand Particles Size Limits

Soil	Particle Size Limit (mm)
Sand	0.074 - 5
Silt	0.002 – 0.074
Clay	< 0.002

Silicates are the common minerals found in soil with clays and non-clays are being silicates. For clays, they have small particle sizes (< 0.002mm) and their cells have a residual negative charge that is balanced by absorbing cations from solution (this has an effect on soil engineering properties such as swelling potential and erosion) (Arulanandan, 2003). Non-clays are considered inert with weak cohesive forces, larger particle sizes and little or no reaction to pore fluid (Liu, (2007).

2.2.2 Water Composition

Like any other substance on earth, water consists of elements (hydrogen and oxygen. The proportion of other constituents like salts and other minerals determines the form in which

water exist. This can determine the reaction of water in the presence of other mixtures as well as affect the properties of water. For example, salt water tends to increase soil salinity when mixed with soil (the amount of salt present in soil) (Arulanandan, 2003). Saltwater (also known as seawater) is water that contains high percentage of dissolved salt, mostly sodium chloride (table salt) other minerals can be present in salt water in varying proportions.

Impurities in water tend to alter its chemical behaviour. Distilled water & deionised water are forms of water than contains a high degree of purity. While distilled water is obtained from distillation to free the water from dissolved salts and other compounds, de-ionised water has ionic salts (such as sodium, calcium, iron, chlorine and sulphate) removed.

If the presence of dissolved ions in water is a factor that enhances conductivity, the conductivity of salt water should be higher than that of distilled water and de-ionised water.

2.3 Properties of Soil-Water System

The inherent characteristics of soil and water will result in certain properties exhibited by a soil-water system. (Yen, 2013) Highlighted that the interactions in the soil-water interface plays a major role in soil behaviour with soil behaviour in the presence of electric fields not only dependent on the significant properties of the individual constituents of the soil mass but also properties of the mass that result from the arrangement of the particles of the mass. For a given sample of soil, the particle size distribution, water content, mineral structure of the soil, the characteristics of the pore fluid as well as the ion exchange reaction determines the properties of the soil system. Some of these properties of soil include physical properties (texture, water content, and density), electrical properties (electrical conductivity and dielectric constant) etc.

2.3.1 Physical Properties of Soil

These properties are of particular importance to the environmental engineers and in agricultural practices, the texture of soil and soil colour are vital physical properties of soil. They affect absorption and radiation of energy. Also sand, silt and clay have different pore spaces between grains of respective soil samples, with pore spaces in sand more than that of silt and clay, therefore, having a degree of permeability decreasing from sand, silt to clay. Soil is considered to be anisotropic by nature i.e. some properties of soil (such as permeability, compressibility, swelling potential) when measured horizontally and vertically are not the same (Arulanandan, 2003).

Soil water content is the ratio of the volume of water in a soil sample to the volume of a soil sample; this greatly affects other properties of soil.

2. 4 Dielectric Theory & Measurement Techniques

2.4.1 Dielectric Theory

On application of electric field to a material, it produces a response which can be evaluated quantitatively in terms of the capacitance, which can be described as a measure of charge retention capacity/ energy stored in a medium. This can be expressed in terms of how easy it is for the molecules of the medium to be polarised and aligned to the electric field applied.

For water (with relatively large dielectric permittivity, 79-81), this is due to the ability of water molecules to align its dipole moments along with an applied field. Different materials exhibit varied dielectric behaviour depending on several conditions of measurement.

The dielectric property of a medium is expressed in terms of the dielectric permittivity, it is a complex quantity expressed as (Cameron, 2007):

$$\varepsilon = \varepsilon' - j\varepsilon'' = \varepsilon_r\varepsilon_o(1 - jtan\delta) \quad (2.1)$$

Where the real part, ε' , is the dielectric permittivity, indicates the amount of storage of charges (stored energy) due to the polarisation of the medium. The imaginary part, ε'', indicates the loss caused by delay in response to the applied field (polarisation loss and conduction loss). ε_r and ε_o are relative and absolute permittivity respectively.

The energy dissipation in the medium can be represented by the loss angent, δ, or dissipation factor, D. This defines the relative 'lossiness' of the medium.

$$\text{Loss tangent, } \delta \text{ or } D = \frac{\varepsilon''}{\varepsilon'} \quad (2.2)$$

2.4.2 Electrical Conductivity

Electrical conduction relates to the ability of the material to conduct electricity through it. For an aqueous solution, this is a measure of the dissolved ions. The higher the dissolved material in water, the higher the conductivity. The direction of movement of ions in a soil-water system or any solution follows the direction of electric current and the electromagnetic field.

2.4.3 Dielectric Permittivity Measurement Techniques.

Studies involving the dielectric permittivity of material are important as the knowledge is used in assessing the structure and molecular behaviour of the materials under study (Smyth, 1955). For some materials, the dielectric permittivity, as well as conductivity on application of electric field, is frequency dependent, however materials like Teflon have minimal (weakly) dependence on frequency, this tends to justify why their permittivity value is quoted as fairly constant value irrespective of the frequency of operation, with

several kinds of literature quoting the dielectric constant of Teflon to be 2.0-2.1 (Ehrlich, 1953), (Microwave101, 2017). Most materials have permittivity values at a specified frequency and temperature owing to polarizability properties of the constituents of the material at these frequencies. With a mixture such as soil particles and water with varying polarisation and conductivities, the permittivity value will contribute by the respective independent properties of water and soil.

Over the years, different studies have been carried out to determine the dielectric permittivity of a material, (Santos, 2009), (Wu M. Y., 2000), (Robinson, 2014), (Sheen, 2005), (Sharma, 2013), (Kraszewski, 1992) with each study geared towards understanding the structure and behaviour of the different materials under investigation and with each method having its own various uniqueness and drawbacks. The measurement techniques can be generally grouped into:

a. Frequency domain Method
b. Time-domain Method

For techniques using frequency domain methods, they can be further categorised into non-resonant and resonant methods. With the formal being as a result of the reflection or transmission of electromagnetic signals and well suited for broadband measurement. The resonant methods utilise the changes and values of the resonant frequencies, the quality factor of the resonator as well as the coupling as a result of feeding microwave signals to the resonator before or after in introduction of the material sample. The choice of the technique depends on (App. Note, 2006)

- The frequency of interest

- The expected value of the dielectric permittivity ($\varepsilon' \; and \; \varepsilon''$)
- The material properties (homogenous, isotropic, anisotropic, heterogeneous etc.)
- The material form (i.e. liquid, powder, solid, sheet)

At radio frequencies and microwave frequencies, the dielectric properties of granular materials depend on the frequency, the amount of water present, bulk density, and temperature (Guo, 2013) . Due to the polar nature of water, at these frequencies, water is the most important factor. This is because other factors such as bulk density and temperature are water related. Temperature change affects the energetic status of the water molecules.

i. Parallel plate capacitor

In this technique, parallel plates are used as the sample holder with the material under testing, sandwiched between the plates. It requires an impedance analyser or LCR meter. The measurement using this method are at low frequencies, typically below 1 GHz. (App. Note, 2006), (Arulanandan, 2003) The measured capacitance between the plates of certain cross-sectional area separated by a given distance is used to calculate the dielectric constant.

$$C = \frac{A\varepsilon'}{t} \tag{2.3}$$

C = Capacitance

A = Cross- Sectional Area of the Plates

t = Distance Separation between the plates

ε' = Dielectric permittivity

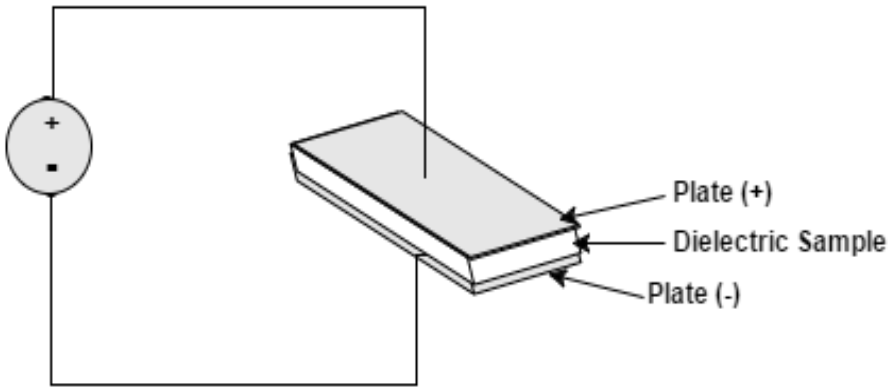

Figure 2:1 Parallel Plate Capacitor

ii. Transmission/reflection line method

This involves placing the material under testing in a section of a waveguide or coaxial line and the two-port complex scattering parameters (S_{11} for Reflection Method, S_{21} for Transmission Method) are measured with a Vector Network Analyzer, VNA. The relevant Scattering parameters (S_{11} or S_{21}) relates to the complex permittivity. This can be used to obtain the real part of the dielectric permittivity of high or low loss material specimen but lack the capability to measure accurate loss tangent (App. Note, 2006).

These methods are suitable for broadband measurements as well as homogenous material with the ability to machine a sample to be placed in a transmission line. According to (Baker-Jarvis, 1990), air gap between samples and the walls of the transmission line (waveguide/coaxial line) among other factors, restricts the accuracy of results using this method. It is well suited to obtain the real part of the dielectric permittivity. It lacks the capability to measure accurately loss tangent of a dielectric. (Kaatze, 2010).

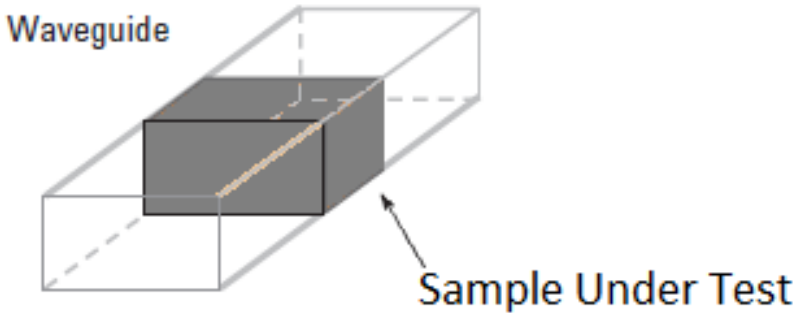

Figure 2:2: Material under Test Placed in Waveguide in a Transmission/Reflection Technique

iii. Coaxial probe method

This method involves a cut-off section of a transmission line-an open-ended coaxial probe. The dielectric material is tested by touching the probe with it or immersing the probe in a liquid. The field at the probe end infringes into the dielectric sample and the reflected signal is measured using a vector network analyser, VNA. The reflected signal (S_{11}) is used to relate to the dielectric permittivity.

The use of coaxial probe method for measurement of dielectric permittivity was investigated by (Santos, 2009), (Wu M. Y., 2000) and also described in (App. Note, 2006). It was shown that this method is well suited for determining the dielectric permittivity of liquid and powdered samples (semi-solids).

iv. Free space method

This is used for testing of dielectric materials under high temperature or hostile environment. The materials are separated from the test apparatus. With two facing antennae connected to a vector network analyser with the material sample placed between the

antennae. (Ghodgaonkar, 1989) Applied this technique in measuring the permittivity of ceramic slabs at the frequency range of 14.5-17.5 GHz. The material sample is placed with a plate between the two antennae. According to (Ghodgaonkar, 1989), inaccuracies of this method are due to diffraction the edges material sample interface and multiple reflections between the antennae

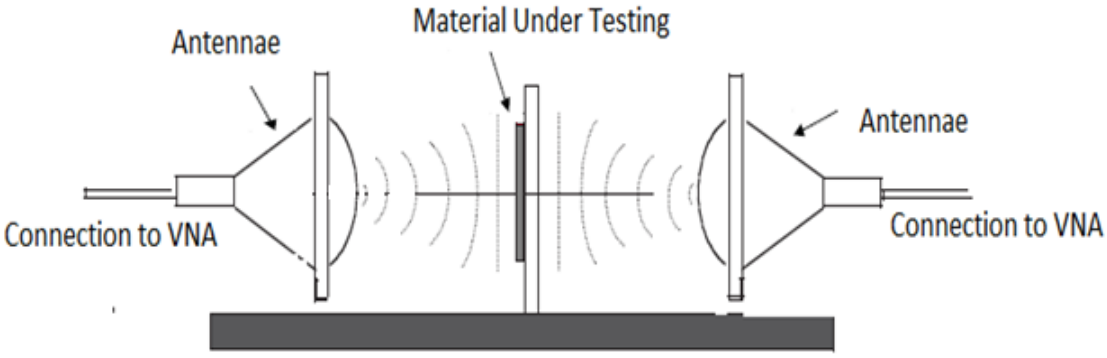

Figure 2:3: Setup for Free Space Measurement [Source: **(App. Note, 2006)**]

v. Resonant method

For measurement at single frequencies and low loss materials, the resonance technique is suitable as it can determine dielectric permittivity of materials at specific frequencies. One of the advantage of this method is that the electromagnetic field is confined within the material and/or cavity thereby making it less susceptible to external losses. Measurement using the resonance theory have been widely reported. (Sheen, 2005) Explained the various resonance techniques with some having a set-up in which the resonance is primarily supported by the dielectric material. The metal shield present in this set up is basically to prevent radiation losses. This method is referred to as dielectric resonance technique. The fields are confined to the dielectric material.

Also, in cavity perturbation technique, the resonance is dictated by the metal cavity itself, the perturbation of fields in the cavity is caused by the introduction of a small sample of dielectric material. This change in field distribution as a result of the dielectric is used to characterise the dielectric permittivity and dielectric loss of the sample. In this technique, the volume of the resonator cavity and the volume of the sample are important in determining the dielectric properties of the sample as well as the quality factor before and after the introduction of the material sample. Also, to determine the electrical properties, the sample is placed in regions of the maximum electric field. In ensuring the accuracy of this method, the perturbation caused by the dielectric sample has to very small and this is achievable if the volume of the sample is very small as compared to the volume of the cavity. (Kraszewski, 1992), (Sharma, 2013) and several other researchers have made improvements to this technique.

The table below is a summary of some of the techniques for determining the permittivity of a materials.

Table 2.2: Summary of Dielectric measurement Techniques

S/N	Measurement Techniques	Principles	Applications, Advantages & Disadvantages
1	Parallel Plate (App. Note, 2006), (Arulanandan, 2003) (Jha, 2011)	Permittivity is obtained from capacitance obtained between parallel plates.	Best for low frequencies measurements; thin and flat sheets
2	Transmission/Reflection (App. Note, 2006) , (Hengcharoen, 2011) (Kaatze, 2010), (Jha, 2011), (Baker-Jarvis, 1990)	Permittivity is obtained from measurement of scattering parameters ($S_{11}\ and\ S_{21}$).	• Broadband measurements • Machinable samples • Lacks the capability to measure loss tangent • Less accurate
3	Coaxial Probe (App. Note, 2006), (Santos, 2009), (Wu M. Y., 2000), (Jha, 2011)	Permittivity is obtained from reflected (S_{11}) signal from a probe	• Broadband measurements • Well suited for liquids and powders (semi-solids)

4	Free Space (Ghodgaonkar, 1989), (Trabelsi, 2003), (Jha, 2011)	Material under test is placed between two microwave antennae facing each other	• Applicable under high temperatures or hostile environment. • Inaccuracies are due to diffractions and multiple reflections. • Well suited for slabs like ceramics
5	Resonant– Cavity Perturbation (Sheen, 2005), (Kraszewski, 1992), (Li, 2001), (Jha, 2011) (Sharma, 2013)	The change in field distribution as a result of introduction of dielectric sample is used to characterise the permittivity values.	• Measures at single frequency. • EM Fields are confined within the resonator and sample. • Less prone to external losses and most accurate. • Sample volume and positions must be considered

Accurately estimating and positioning the volume of the sample in the cavity perturbation technique so as to cause the desired perturbation of fields in the cavity for some samples like liquids and mixtures can be difficult and when such samples need to be placed in a container so as to localise their positioning in the cavity to positions of maximum fields, analysis has to be performed so as to eliminate the effect of the properties of the container holding sample, and this can be complex. However, reasonable research work has been carried out for samples of defined volume and shape using this technique which have been widely accepted. Also, for measurements at multiple frequencies, the geometry of the cavity is altered.

2.5 Transmission Line Theory

Propagation of electromagnetic fields in various transmission lines is usually in different modes. These can be in the transverse electromagnetic mode (TEM) or an infinite number of Electric Field (**E)** and magnetic Field (**H)** mode. For cables like coaxial cables, the dominant mode is TEM (it has neither magnetic nor electric field in the direction of propagation).

For any of the modes, the propagation constant in free space is given by:

$$\gamma_t = \frac{2\pi}{\lambda_0}\left[\left(\frac{\lambda_0}{\lambda_c}\right)^2 - \varepsilon\right]^{1/2} \quad (2.4)$$

Where λ_0 and λ_c is the wavelength of free space and cut-off wavelength respectively. For a TEM mode, the cut-off wavelength is equal to infinity, however this is finite for other modes. ε is the complex permittivity as depicted in equation (1.1), therefore, for a TEM transmission line (e.g. coaxial cable) we have:

$$\text{Propagation Constant (TEM), } \gamma_t = j\,\omega\sqrt{\mu\varepsilon} \quad (2.5)$$

Shorting ends of a metal structure, thereby confining electromagnetic fields in it forms a cavity which resonates (when stored electric field equals magnetic field) at certain frequencies. Using lumped elements, the resonating structure can be modelled as an LC circuit depicting a lossless case or RLC for a lossy resonating structure where R (resistance) accounts for the losses in the walls of the resonator and the dielectric losses associated with the material inside the conductor. L (inductance) and C (capacitance) determine the resonant frequency of the resonator.

With distributed elements (waveguide, coaxial, microstrip etc) the length of the resonator is in multiples of quarter wavelength of the desired resonant frequency, as such in choosing the physical length of the resonator, the resonant frequency is considered (Pozar, 2009).

One of the advantages of using distributed elements as against RLC circuits for resonator designs is to achieve higher quality factor, Q, and minimise losses

The ability of the transmission line to support electromagnetic waves results in characteristic impedance and the phase constant which are both functions of the dielectric permittivity of the material in the transmission line.

The characteristic impedance of a coaxial cable is given by:

$$Z_t = \frac{j\omega\mu}{2\pi\gamma} \ln \frac{b}{a} \tag{2.6}$$

γ is given in equation (2.5).

Resonators require a form of excitation by coupling energy into them via an external coupling. This can be done by

a.) Coupling using an electric probe: This is modelled as a capacitance
b.) Coupling using magnetic probe: This acts as an inductance
c.) Coupling using Gap/Distance: This is modelled as capacitance because of the metallic surfaces between the resonator and the external coupling system. The distance between the metallic openings determines the coupling capacitance.

A parameter to measure the degree of coupling between the resonator and the external coupling system is denoted as the coupling coefficient, K.

2.5.1 Equivalent Circuit Model

The behaviour of transmission lines can be well represented using lumped elements. (Pozar, 2009) Contains vast literature of transmission lines models for both lossless and lossy transmission lines.

The lossless and lossy models for transmission lines are depicted below:

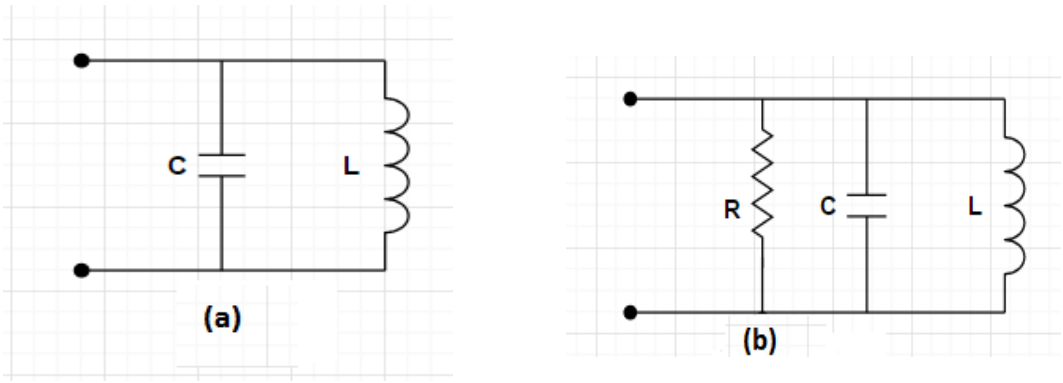

Figure 2:4: Equivalent model of resonator- (a) Lossless (b) Lossy

2.5.2 Quality Factor

The losses associated with a resonator can be contributed by the metal wall conductivity, the dielectric contained in the resonator, coupling to the resonator; quantified as quality factor of the resonator. It can be used to predict how difficult and/or easy it is to inject a signal whose frequency is different from the resonant frequency of the resonator device. High quality factor indicates high accuracy and narrow bandwidth in relation to the energy stored with respect to the power dissipated in the resonator.

Different methods have been proposed for determining the unloaded quality factor with some requiring measurement as well as reading information from a smith chart, some methods having limitations. Reading off data from the smith chart so as to extrapolate the loaded quality factor can be cumbersome and this can be prone to errors especially for novice users. Also, quality factor can be expressed in terms of the resonance frequency and the 3-dB bandwidth of the impedance plot. (Drozd, 1996) proposed a method of determining quality factor using S-parameter data. This has been found to be useful for both transmission lines, resonators and applications with low and high quality factors, however, this process involves several mathematical steps which one has to follow to obtain the desired quality factor. Quality factor can be expressed as:

- The Unloaded Quality Factor, Q_u, which is a characteristic of the resonating device itself
- The External Quality Factor, Q_e, this expresses the coupling condition between the external circuit and the resonating device itself.
- Loaded Quality Factor, Q_L, This is a contribution of the external quality factor and the unloaded quality factor

Equation (2.7) relates the unloaded Q, the External Q and the Loaded Q.

$$\frac{1}{Q_L} = \frac{1}{Q_u} + \frac{1}{Q_e} \tag{2.7}$$

To estimate the losses associated with a resonator, the dielectric loss tangent is related to the Unloaded Quality factor, Q_u using equation (2.8)

$$Q_u = \frac{1}{tan\,\delta} \tag{2.8}$$

Equation (2.8) holds if the resonator is lossless (when the walls of the resonator have infinite conductivity).

Considering metallic losses,

$$\frac{1}{Q_u} = \frac{1}{Q_c} + \frac{1}{Q_d} \tag{2.9}$$

Where, Q_c is the quality factor due to the conductivity of the metallic walls, Q_d is the quality factor due to the dielectric. Therefore,

$$Q_d = \frac{1}{tan\,\delta} \tag{2.10}$$

For a coaxial cable, Q_c is given by;

$$Q_c = 2\frac{\sqrt{\pi.f.\sigma}\ln\left(\frac{b}{a}\right)}{\frac{1}{a}+\frac{1}{b}} \tag{2.11}$$

Where σ = conductivity of the conductor (S/m)

a and *b* are the radii of the inner and outer conductors respectively

f is the frequency of measurement

The external coupling to the resonator allows for the excitation of the electromagnetic fields in the cavity. Depending on the value or the extent of coupling, the resonant frequency of the resonator tends to vary, this factor that defines the extent of coupling is termed coupling coefficient. A given resonant circuit can have a coupling coefficient, K , where $1 \leq K \leq 1$. That is; under-coupled (coupling coefficient < 1), critically coupled (coupling coefficient =1), over-coupled (coupling coefficient> 1).

Depicting a coupled circuit with figure 2.5 below, where Z is the impedance of the coupling circuit, the coupling coefficient is given as:

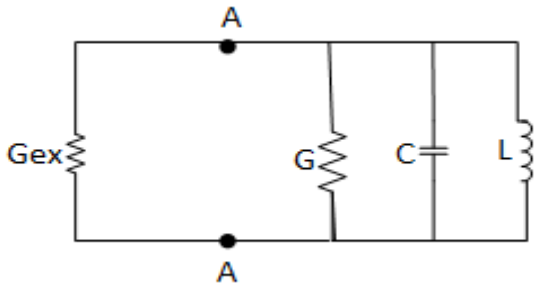

Figure 2:5: Coupled Resonator

$$K = \frac{Power\ Dissipated\ in\ the\ external\ load}{Power\ Dissipated\ in\ the\ resonator} = \frac{G_{ex}}{G} = \frac{Q_u}{Q_{ex}} \qquad (2.12)$$

In reality, the coupling circuit has an impedance value comprising the resistive and the reactive component (Z = R + jX). However, this depends on the mode of coupling; inductive coupling (using a magnetic loop) or capacitive coupling (using probe or gap). According to (Chua, 2003) and (Cameron, 2007), a resonator coupled to an input port can be accurately modelled accounting for coupling losses using a reactive component, for a capacitively coupled resonator, the equivalent circuit is:

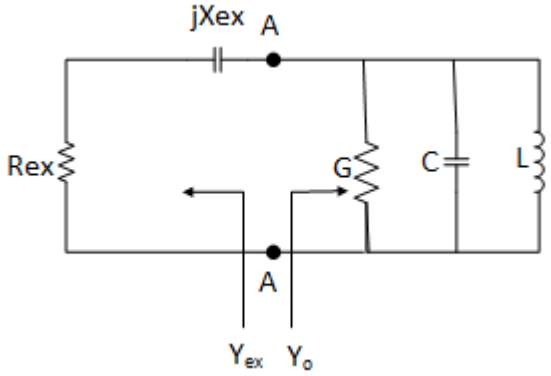

Figure 2:6: Capacitively Coupled Resonator at the input port

For an uncoupled lumped element resonant circuit given in Fig 1.4(b), the unloaded quality factor is given as:

$$Q_u = \frac{\omega C}{G} \tag{2.13}$$

The input impedance looking towards the resonator, $\mathbf{Y_o}$, is given by:

$$Y_o = G\left(1 + jQ_u\left(\frac{\omega}{\omega_0} - \frac{\omega_0}{\omega}\right)\right) \tag{2.14}$$

Where G = Conductance ($\frac{1}{R}$)

Considering Fig 2.6, the admittance looking towards the source from point A:A is given by (Cameron, 2007):

$$Y_{ex} = \frac{1}{R_{ex} + jX_{ex}} \tag{2.15}$$

X_{ex}= Reactance due to capacitive coupling

Due to the loading as result of X_{ex}, the resonant frequency is reduced from ω_o $\left(\frac{1}{2\pi\sqrt{LC}}\right)$ to a value ω_L, this holds when X_{ex} capacitive reactance is. For inductive reactance, is $\omega_o < \omega_L$.

For simplification, Norton equivalent circuit of Fig 2.6 is given by:

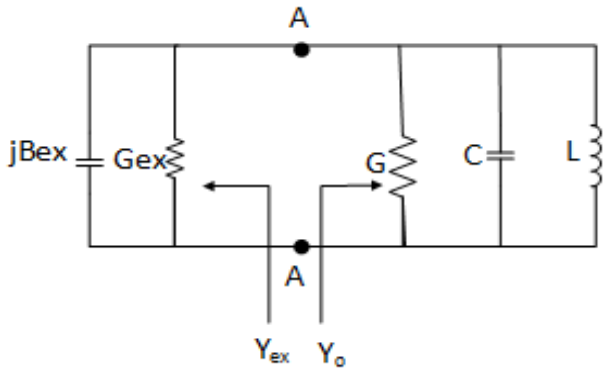

Figure 2:7: Equivalent Circuit for Capacitive Coupled Resonator

B_{ex} = Susceptance due to capacitive coupling

Therefore, equation (2.15) becomes

$Y_{ex} = G_{ex} + jB_{ex}$

The loaded input impedance, $Y_L = Y_{ex} + Y_o$ (2.16a)

$$\text{Where, } Y_o = G\left(1 + jQ_o\left(\frac{\omega}{\omega_0} - \frac{\omega_0}{\omega}\right)\right)$$

Therefore, equation (2.16a) becomes:

$$Y_L = G_{ex} + jB_{ex} + G + jGQ_o\left(\frac{\omega}{\omega_0} - \frac{\omega_0}{\omega}\right) = G_{ex} + G + j\left(B_{ex} + GQ_o\left(\frac{w}{w_0} - \frac{w_0}{w}\right)\right) \quad (2.16b)$$

The loaded quality factor is given by equation (2. 17) which can be expressed in terms of the unloaded quality factor using equation (2.13)

$$Q_L = \frac{\omega C}{G_{ex}+G} \quad (2.17)$$

$$Q_L = Q_o \frac{G}{G_{ex}+G} = Q_o \frac{1}{\frac{G_{ex}}{G}+1}$$

The coefficient of coupling is expressed in equation (2.12) as the ratio of $\frac{G_{ex}}{G}$,

Therefore,

$$Q_L = \frac{Q_o}{1+k} \tag{2. 18}$$

2.4.6 Group Delay

The group delay is the rate change of the phase angle with respect to the frequency. For a coupled resonator, it can be considered as the time taken for microwave energy to get in and reflected out of the resonator (when the reflected group delay is considered). Considering the input reflected signal, the group delay is the rate of change of the phase of the input reflection coefficient (S_{11}) with frequency, signifying extent to which the phase of the input reflection coefficient is distorted. A signal with a linear phase has minimal distortion, hence constant group delay.

$$\Gamma_d = -\frac{\delta\phi}{\delta\omega} \tag{2.19}$$

The method of applying group delay technique has been used in filter technology. It has been found to be useful in filter design optimisation with considerable inputs from (Ness, 1998) who proposed that the group delay of the reflected signal contains all the information needed to design and tune filters providing an easy method for measuring the key elements of a filter. Ness also emphasised that the importance to keep the reflected group delay response symmetric about the centre frequency, but further research work has proven that this is difficult for response with a wider bandwidth. (Laforge, Mansour, & Yu, 2010)

Further showed that the group delay response is only symmetrical for designs with narrow bandwidth.

Considering a lossless LC circuit modelled as a resonator coupled to an input source, the input admittance.

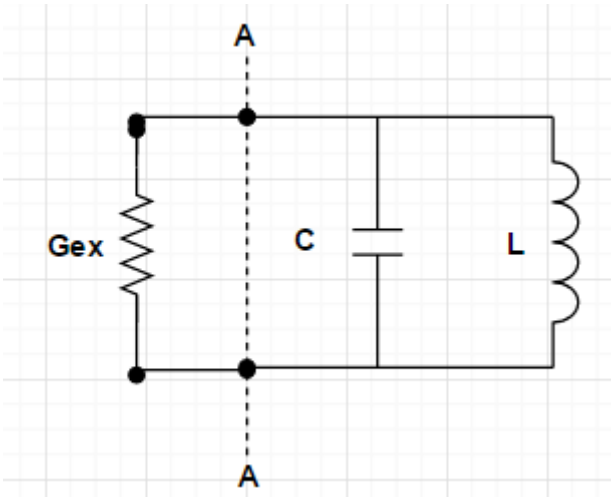

Figure 2:8: Coupled lossless LC circuit

The input admittance at A: A,

$$Y_{in} = j\omega C + \frac{1}{j\omega L} = j\omega_o C \left(\frac{\omega}{\omega_o} - \frac{\omega_o}{\omega}\right) \quad (2.20a)$$

ω_o is the resonant frequency, at frequency close to the resonant frequency, $\omega = \omega_o + \Delta\omega$, therefore,

$$Y_{in} \approx j\omega_o C \left(\frac{2\Delta\omega}{\omega_o}\right) \quad (2.\ 20b)$$

The input coupling is represented by the conductance, G_{ex}, and the input reflection coefficient at the section A:A is given by (Ness, 1998):

$$S_{11} = \frac{Gex - Y_{in}}{Gex + Y_{in}} \tag{2.21}$$

$$= \frac{1 - \frac{Y_{in}}{Gex}}{1 + \frac{Y_{in}}{Gex}} = \frac{1 - \frac{j\omega_o C\left(\frac{2\Delta\omega}{\omega_o}\right)}{Gex}}{1 + \frac{j\omega_o C\left(\frac{2\Delta\omega}{\omega_o}\right)}{Gex}} \ ,$$

The phase of the input reflection coefficient is given by:

$$\phi = -2\arctan\left(\frac{\omega_o C\left(\frac{2\Delta\omega}{\omega_o}\right)}{Gex}\right) \tag{2.22a}$$

But the external quality factor $Q_e = \frac{\omega C}{Gex}$

$$\phi = -2\arctan\left(Q_e\left(\frac{2\Delta\omega}{\omega_o}\right)\right) \tag{2.22b}$$

From equation (1.19)

$$\Gamma_d = -\frac{\delta\phi}{\delta\omega} = \frac{\delta}{\delta\omega}\left(2\arctan\left(Q_e\left(\frac{2(\omega-\omega_o)}{\omega_o}\right)\right)\right)$$

$$\Gamma_d = \frac{4Q_e}{\omega_o}\frac{1}{1+\left(\frac{2Q_e(\omega-\omega_o)}{\omega_o}\right)^2} \tag{2.23a}$$

From equation (2.23a), the group delay of the input reflection coefficient at the resonant frequency for a single resonator is given by:

$$\Gamma_d = \frac{4Q_e}{\omega_o} \tag{2.23b}$$

From equation (2.23b), the external quality factor can be evaluated using the group delay information of the reflected input signal.

Chapter 3 **: Coupled Resonator**

3.1 Introduction

The chapter presents the concept behind the design of a gap-coupled coaxial resonator using group delay method. It considers the model of resonators using lumped elements with a lossless transmission line represented as LC circuit and a lossy transmission as an RLC circuit. Equations are derived for the impedance/admittance of the coupled resonator which is affected by the coupling to the resonator, and the amount of loss in the resonantor. Evaluation of the input impedance/admittance is useful in the group delay equations since group delay is related to the phase of the input reflection coefficient. The coupling capacitance and the dielectric permittivity of a given sample are therefore extracted from the group delay equation of a gap-coupled resonator.

3.2 Lossless Coupled Resonator Using Lumped Elements

For an uncoupled LC resonator, given in Fig (2.4), the resonant frequency, ω_o, is a function of the values of the inductor and the capacitance, with the resonator frequency given as

$$f_o = \frac{1}{2\pi\sqrt{LC}} \tag{3.1}$$

Capacitive or inductive coupling loads the resonator and this results in a shift in resonant frequency. Achieving under-coupled, over-coupled or critically coupled is also a function of the inductance or the capacitance value contributed by the coupling and the resistance of the resonator. For cases where maximum power transfer is required, critically coupling is desirable. A lossless coupled resonator is basically an over-coupled and has an infinite value of unloaded quality factor.

3.3 Lossy Coupled Resonator

Typically, the value of the resonant frequency of a lossless coupled resonator is the same as that of a lossy one assuming for an RLC lumped element the values of the inductance and the capacitance are the same. This is shown by the plots in Fig. (3.2) and Fig. (3.4).

Depending on the coupling to be achieved, a relatively higher coupling value is needed for a lossy resonator if it is to be driven to either its critical state where the amount of energy stored in the resonator is equal to the power dissipated or over-coupled state where the energy stored in the resonator is greater than the power dissipated.

3.4 Input Impedance/Admittance of a Coupled Resonator

3.4.1 Lumped RLC Circuit

For a simple lossless parallel LC circuit, the input impedance at resonance is very high, $Zin|_{\omega o} \rightarrow \infty$ (admittance $Yin|_{\omega o} \rightarrow 0$), shown in Fig (3.2)

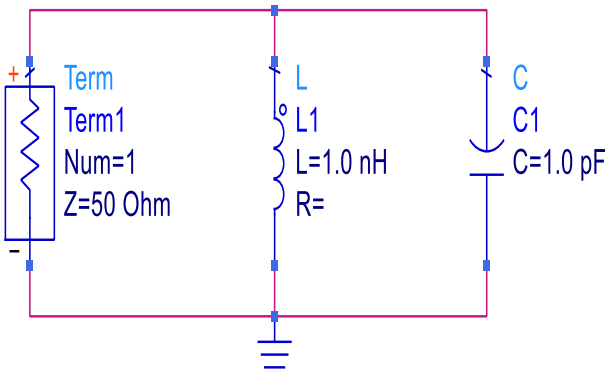

Figure 3:1: Lossless LC Resonator

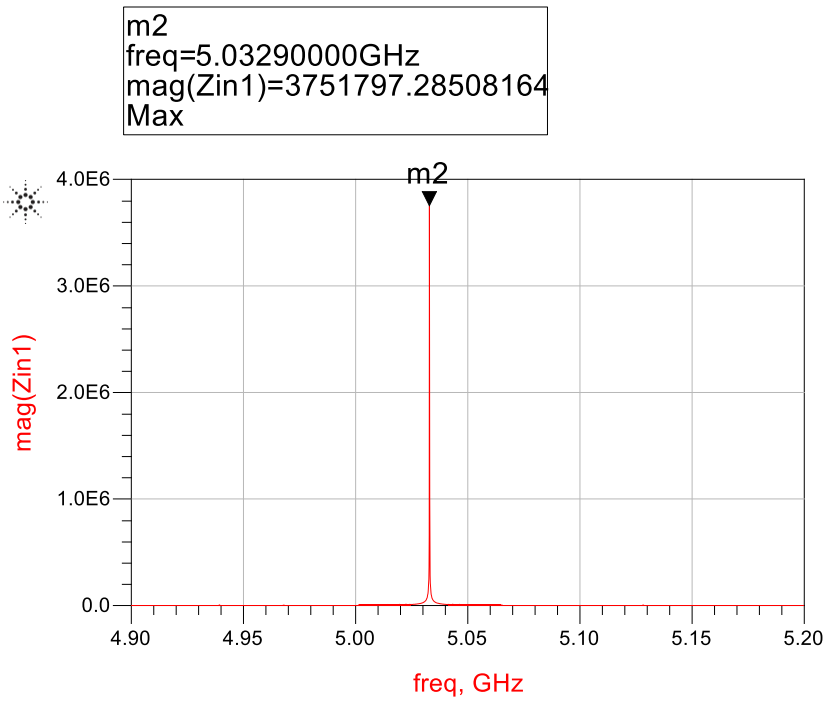

Figure 3:2: Plot of Input impedance of a Lossless LC Resonator

Considering Fig (3.1) and Fig (3.2),

$$\text{Input admittance } Y_{in} = j\omega C + \frac{1}{j\omega L} \qquad (3.2a)$$

But, from equation (3.1), $\omega_o = \frac{1}{\sqrt{LC}}$

$\omega_0^2 = \frac{1}{LC}$

$$Y_{in} = j\omega C - j\frac{\omega_0^2 C}{\omega} = j\omega_o C\left(\frac{\omega}{\omega_o} - \frac{\omega_o}{\omega}\right)$$

But, $\left(\frac{\omega}{\omega_o} - \frac{\omega_o}{\omega}\right) = \frac{\omega^2 - \omega_0^2}{\omega\omega_o}$,

Taking $\omega^2 - \omega_0^2 = (\omega - \omega_o)(\omega + \omega_o)$

Where $\Delta\omega = \omega - \omega_o$

Hence, $\omega^2 - \omega_0^2 = \Delta\omega(2\omega - \Delta\omega)$

When ω *approaches* ω_o (for small changes in $\Delta\omega$), $(\frac{\omega}{\omega_o} - \frac{\omega_o}{\omega}) \approx 2\frac{\Delta\omega}{\omega_o}$

$$Y_{in} = j\omega_o C(\frac{\omega}{\omega_o} - \frac{\omega_o}{\omega}) = j\omega_o C\ (2\frac{\Delta\omega}{\omega_o})$$

$$Y_{in} = jC\ 2\Delta\omega\ |_{\omega \to \omega_o} \qquad (3.2b)$$

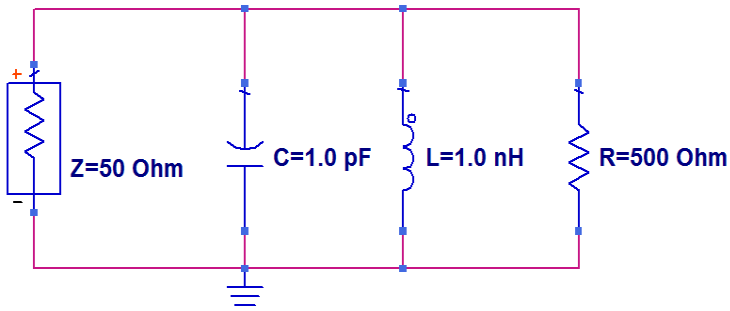

Figure 3:3: RLC lumped element Resonator

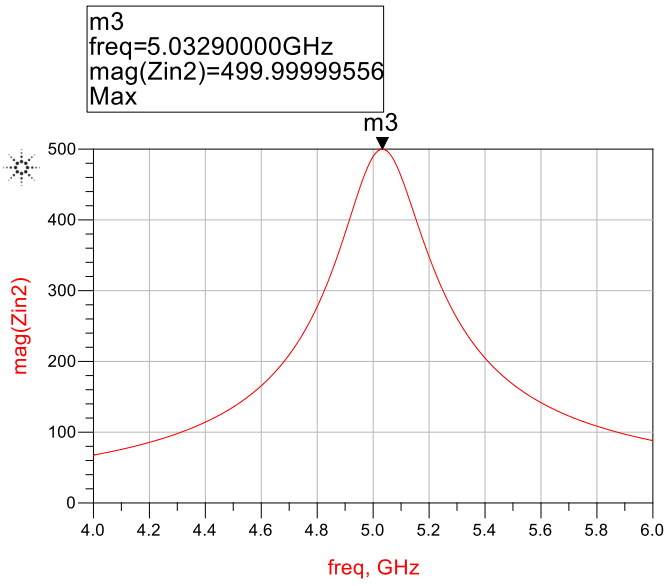

Figure 3:4: Plot of Input impedance of RLC lumped element Resonator

Considering RLC circuit in Fig (3.4),

$$Z_{in} = \left(\frac{1}{R} + j\omega L + \frac{1}{j\omega C}\right)^{-1} \tag{3.3}$$

The input impedance at resonance equals the value of the R (resistance) as seen in Fig (3.4) , m3, this sometimes plays a role in the amount of energy coupled to the resonator.

3.4.2 Coupled Lumped RLC Circuit

For the coupled resonator, there is observable change in the input impedance at resonance when compared to the uncoupled resonator. For example, series coupling to a resonator using a capacitor results in approximately zero resultant input impedance (for LC circuit) and lowered input impedance (for RLC circuit) at resonance. The new resonant frequency is also lower than that of the uncoupled circuit as shown below:

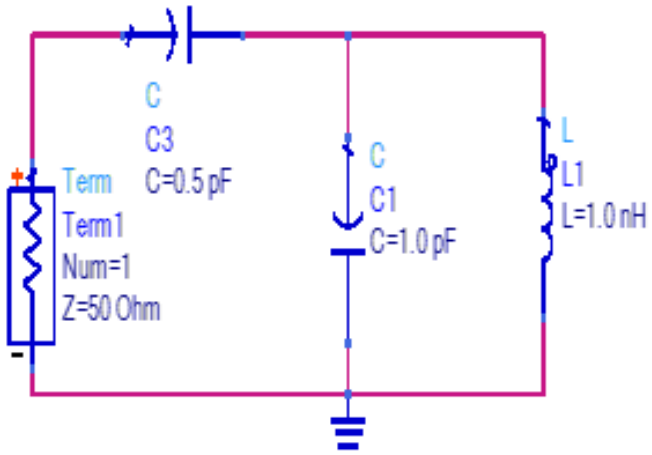

Figure 3:5: Coupled Lossless LC resonator

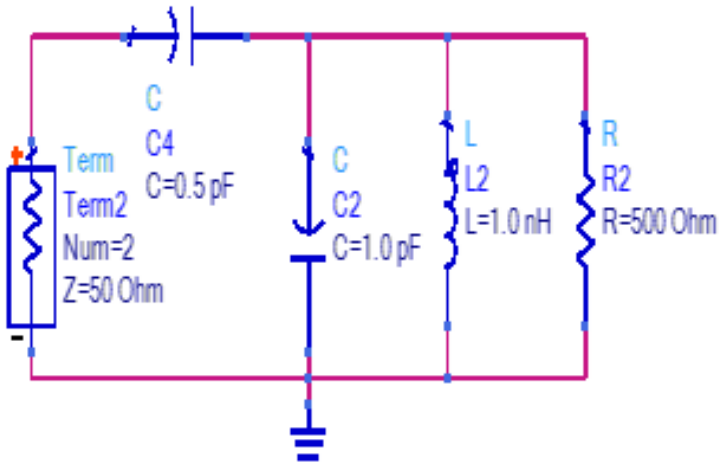

Figure 3:6: Coupled lossy RLC resonator

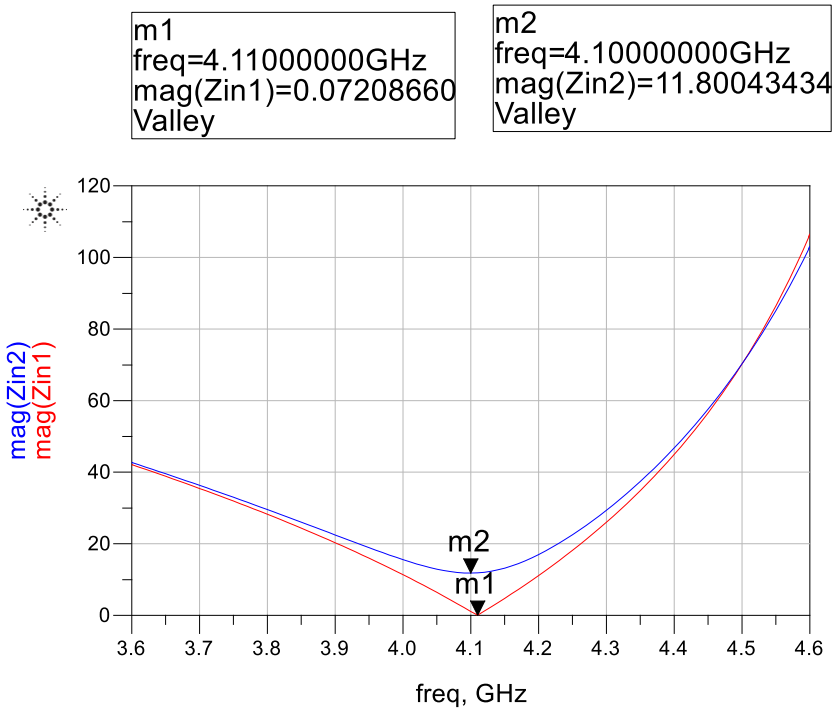

Figure 3:7: Plot of input impedance of a coupled resonator: Red (lossless LC Circuit), Blue (lossy RLC Circuit)

It can be observed from Figure 3.7 that the input impedance at resonance for a RLC circuit (lossy case, m2) is not equal to zero as against LC circuit (m1). According to (Pozar, 2009),

to account for this loss in a lossy resonator using equation (3.2b), the resonant frequency of a lossless resonator (ω_o) can be replaced with a complex resonant frequency when the resonator is lossy using the equation:

$$\omega_o \rightarrow \omega_o \left(1 + j\frac{1}{2Q_u}\right) \tag{3.4}$$

Where Q_u = Unloaded quality factor of the resonator.

Considering equation (3.2b), modelled as a lossless LC circuit with no Resistor, R. For a lossy circuit represented by Fig (3.3) containing a resistor, R, the equivalent equation in the lossy case for equation (3.2b) can be shown by using equation (3.4) thus:

$For\ lossless\ case,\ Y_{in} = jC\ 2\Delta\omega = jC\ 2\ (\omega - \omega_o)$

But for lossy case ω_o is replaced with $\omega_o \left(1 + j\frac{1}{2Q_u}\right)$

where Q_u is the unloaded quality factor

Therefore,

$$Y_{in} = jC\ 2\Delta\omega = jC\ 2\left(\omega - \omega_o\left(1 + j\frac{1}{2Q_u}\right)\right) = jC\ 2(\omega - \omega_o) + \frac{C\omega_o}{Q_u} \tag{3.4a}$$

From equation (3.4a) above, the term $\frac{C\omega_o}{Q_u}$ is equal to the R, resistance of the circuit (since Q = ω RC). This shows how the resonant frequency of a lossless resonator (ω_o) can be replaced with a complex resonant frequency $\omega_o \left(1 + j\frac{1}{2Q_u}\right)$ when the resonator becomes lossy.

3.4.3 Distributed Transmission line Circuits

Using a short-circuited transmission line, the responses (input impedance and coupling effect) are similar to the parallel RLC lumped element (a quarter wave transmission line is modelled as parallel RLC).

For an ideal transmission line that is capacitively coupled using series coupling, we have for example:

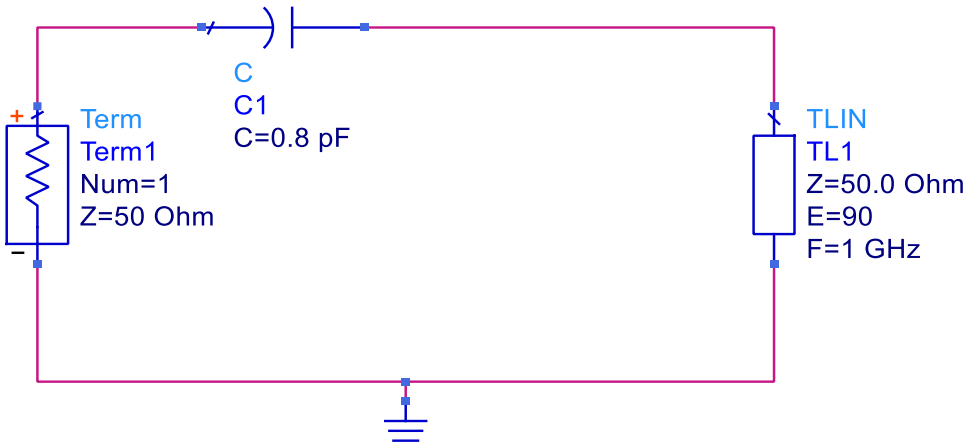

Figure 3:8: Coupled Ideal Quarter-wavelength Transmission Line

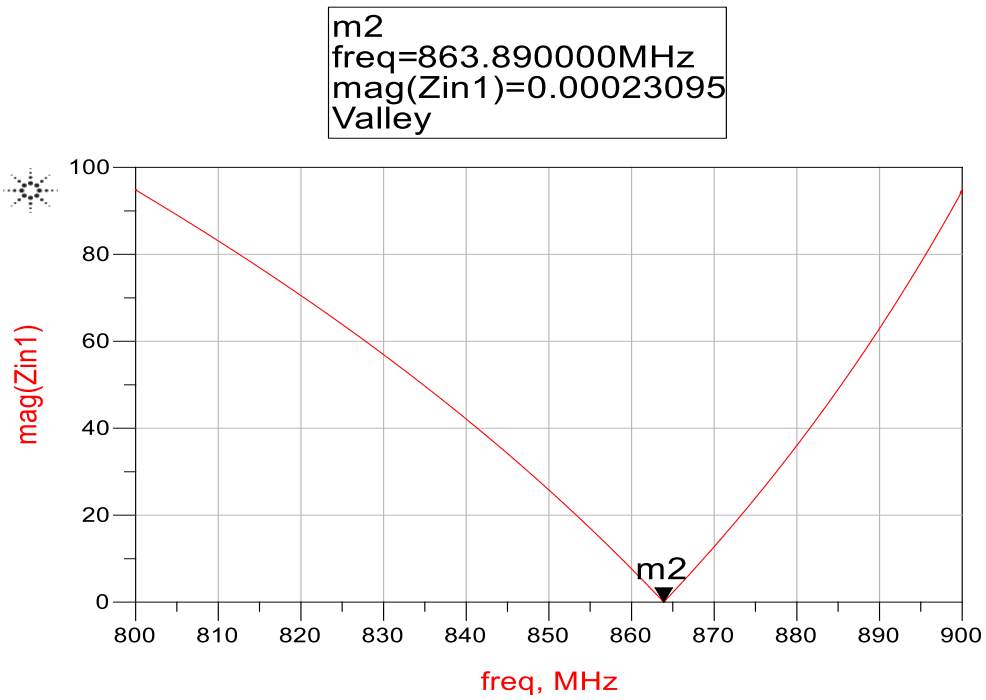

Figure 3:9: Plot of input impedance of coupled ideal Quarter-wavelength Transmission line

The input impedance,

$$Z_{in} = \frac{1}{j\omega C} + Z_t \tan\gamma l = \frac{-j}{\omega C} + Z_t \tan\gamma l \qquad (3.5a)$$

Where γ_t is the propagation constant (containing the attenuation constant, α and phase constant, β) given in equation (2.5).

At resonance, ω_o, $Z_{in} \approx 0$.

Assuming Figure (3.8) is an ideal lossless transmission line, the loss component of the propagation constant (attenuation constant, α = 0) is ignored. Therefore, equation (3.5a) becomes

$$Z_{in} = j\left(Z_t \tan\beta l - \frac{1}{\omega C} \right) \qquad (3.5b)$$

From equation (2.5), $phase\ constant, \beta = \omega\sqrt{\mu\varepsilon'}$,

$Z_{in(lossless)} = j\left(Z_t \tan\left((\omega\sqrt{\mu\varepsilon'})l\right) - \frac{1}{\omega C} \right)$

ε'= dielectric permittivity depicting the real part of equation (2.1)

ε_0 = Permittivity of free space, 8.85 x 10^{-12}F/m

Evaluating equation (3.5b) further and applying Taylor series about the resonant frequency,ω_o, for simplification, we have:

$Z_{in(lossless)} = jZ_t \left(\tan(\beta l) - \frac{1}{\omega C Z_t} \right) = jZ_t \left(\frac{1}{\mathrm{Cot}(\beta l)} - \frac{1}{\omega C Z_t} \right)$

(Pozar, 2009) $Z\ \ in(\omega) = Z_{in}(\omega_o) + (\omega - \omega_o)\frac{dZ_{in}(\omega)}{d\omega}\Big|_{\omega_o} + \ldots\ldots\ldots\ldots$ (3.5c)

Equation (3.5c) is a Taylor series expansion of the input impedance function,Z_{in} given in equation (3.5b), about the resonant frequency, ω_o

From Figure 3.9, it can be observed that for an ideal quarter-wave transmission line, the input impedance at resonance (ω_o) is approximately zero. Therefore, the $Z_{in}(\omega_o)$ term in the series of equation (3.5c) is zero. Equation (3.5c) becomes;

$\approx (\omega - \omega_o)\frac{dZ_{in}(\omega)}{d\omega}\Big|_{\omega_o}$

$\frac{dZ_{in}(\omega)}{d\omega}\Big|_{\omega_o} = \frac{d\ Z_t}{d\omega}\left[\mathrm{j}\ Z_t \left(\frac{1}{cot(\beta l)} - \frac{1}{Z_t \omega C} \right)\right]$

Therefore, equation (3.5c) becomes:

$Z_{in(lossless)}(\omega) = \mathrm{j}\ Z_t \left(\frac{l\sqrt{\mu\varepsilon'}\ cosec^2(\beta_o l)}{cot(\beta_o l)} + \frac{1}{Z_t \omega_o{}^2 \mathrm{C}} \right)(\omega - \omega_o)$,

Where β_o the phase is constant evaluated at the resonant frequency, ω_o

Using the following trigonometric function

$cosec^2x = (1 + cot^2x)$,

We get

$$Z_{in(lossless)}(\omega) = \text{j}\, Z_t \left(\frac{l\sqrt{\mu\varepsilon'}\,(1+ cot^2(\beta_o l)}{cot^2(\beta_o l)} + \frac{1}{Z_t {\omega_o}^2 \text{C}} \right)(\omega - \omega_o)$$

$$Z_{in(lossless)}(\omega) = \text{j}\, Z_t \left(\frac{l\sqrt{\mu\varepsilon'}\,(1+ cot^2(\beta_o l))}{cot^2\left(\left(\omega_o \sqrt{\mu_0\varepsilon_0\varepsilon'}\right)l\right)} + \frac{1}{Z_t {\omega_o}^2 \text{C}} \right)(\omega - \omega_o)$$

But at resonance (Fig (3.9)), equation (3.5b) equals 0

Therefore, $\frac{1}{cot(\beta_o l)} = \frac{1}{Z_t\, \omega_o C}$, at resonance

$$Z_{in(lossless)}(\omega) = \text{j}\, Z_t \left(\frac{l\sqrt{\mu\varepsilon'}\,(1+ (Z_t\omega_o C)^2)}{(Z_t\omega_o C)^2} + \frac{1}{Z_t {\omega_o}^2 \text{C}} \right)(\omega - \omega_o) \qquad (3.5d)$$

Evaluating $(Z_t\omega_o C)^2$ and $(Z_t {\omega_o}^2 \text{C})$ respectively around frequencies in the range of megahertz and few values of gigahertz, and capacitance, C, values that are in the single digits to tens Pico Farads ranges or less, results in a small value with the term $(Z_t\omega_o C)^2$ and reciprocal of $(Z_t {\omega_o}^2 \text{C})$ such that approximating equation (3.5d) results in:

$$Z_{in(lossless)}(\omega) = \text{j}\, Z_t \left(\frac{l\sqrt{\mu\varepsilon'}\,)}{(Z_t\omega_o C)^2} \right)(\omega - \omega_o) \qquad (3.5e)$$

The dielectric permittivity, ε', is both in the numerator of Equation (3.5e) and, Z_t (from equation 2.6). This depends on the dielectric material contained in the transmission line.

However, for higher accuracy, all terms in (3.5d) are retained without rounding to zero and expanding we have:

$$Z_{in(lossless)}(\omega)=\text{j}\, Z_t \left(\frac{l\sqrt{\mu\varepsilon'}}{(Z_t\omega_o C)^2} + l\sqrt{\mu\varepsilon'} + \frac{1}{Z_t\omega_o{}^2\text{C}}\right)(\omega-\omega_o)$$

Expanding with $Z_t, we\ have$

$$Z_{in(lossless)}(\omega) =\text{j}\left(\frac{l\sqrt{\mu\varepsilon'}}{Z_t(\omega_o C)^2} + Z_t l\sqrt{\mu\varepsilon'} + \frac{1}{\omega_o{}^2\text{C}}\right)(\omega-\omega_o),$$

The dielectric permittivity is expressed in relation to the permittivity of free space, ε_0 as relative permittivity, ε_r.

Also, for a nonmagnetic material, permeability is expressed as absolute permeability, μ_0

But $\sqrt{\mu_0\varepsilon_0} = \frac{1}{c}$

Where c = Speed of light ($3\ \text{x}10^8\ m/s$)

Let $\omega C = B_c$

$$Z_{in(lossless)}(\omega) = \text{j}\ \left(\frac{l\sqrt{\varepsilon_r}}{cZ_t(B_c)^2} + \frac{Z_t l\sqrt{\varepsilon_r}}{\text{c}} + \frac{1}{B_c\omega_o}\right)(\omega-\omega_o) \qquad (3.5f)$$

From equation (3.5f), the value of the input impedance at resonance for a lossless coupled transmission line is dependent on the characteristic impedance of the transmission line, Z_t which is a function of the dielectric permittivity of the material contained in the resonator.

The term $\frac{Z_t l\sqrt{\varepsilon_r}}{\text{c}}$ and $\frac{1}{B_c\omega_o}$ in equation (3.5f) when evaluated are very small. However, they are retained for higher accuracy of results.

Let P =$\left(\frac{l\sqrt{\varepsilon_r}}{cZ_t(B_c)^2} + \frac{Z_t l\sqrt{\varepsilon_r}}{\text{c}} + \frac{1}{B_c\omega_o}\right)$, in equation (3.5f)

And considering a non-ideal transmission line with losses either from the conductor or the dielectric contained in the resonator, the resonant frequency, ω_o term in ' $\omega - \omega_o$' in equation (3.5f) is replaced with $\omega - \omega_o(1 + j\frac{1}{2Q_o})$, therefore the input impedance becomes:

$$Z_{in(Lossy)}(\omega) = \text{j}\ P\left(\omega - \omega_o\left(1 + j\frac{1}{2Q_u}\right)\right) = \text{j}P(\omega - \omega_o) + \frac{P\omega_o}{2Q_u} \qquad (3.5g)$$

It is assumed that ω_o term in P is retained when the resonator is lossy for easy of mathematical evaluation. This assumption is valid and account for high accuracy of Z_{in} at higher loss tangent values in Table (3.1)

Also for simplification using notations P and R, equation (3.5g) can be expressed as

$$Z_{in(Lossy)} = \text{j}P(\omega - \omega_o) + R \qquad (3.5h)$$

Where R = $\frac{P\omega_o}{2Q_u}$

Considering the circuit below, equation (3.5f) is used to compare values of input impedance (simulated and calculated) at resonance for a coaxial model with certain dielectric constant and loss tangent values. This will help to validate the equation when compared to the simulated values.

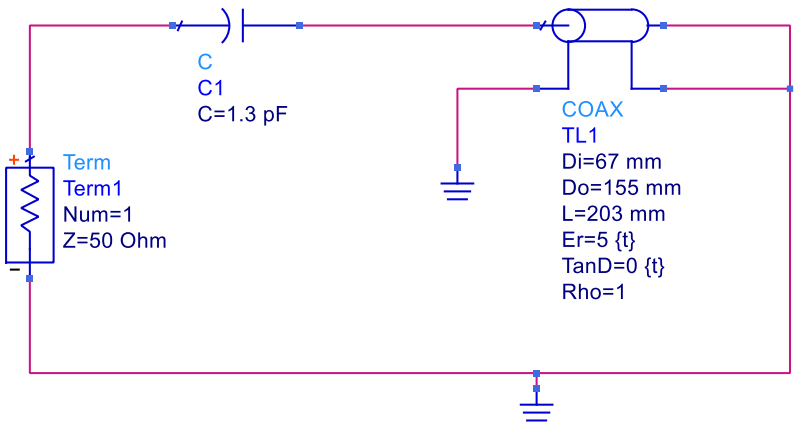

Figure 3:10: Coupled Coaxial Resonator Model

Table 3.1: Simulated and calculated input impedance for a coupled resonator containing sample a dielectric sample

S/N	$\varepsilon_{r\,\text{simulated}}$	$tan\delta_{\text{simulated}}$	Z_{in}simulated @ ω_o	Z_{in}calculated @ ω_o	% Difference between Z_{in}simulated & Z_{in}calculated
1	5	0.0000	2.87271437	2.7583268	3.9620%
2	5	0.0001	4.75018886	4.564280316	3.9137%
3	5	0.0005	12.2981838	12.25844153	0.30614%
4	5	0.0008	18.02384955	18.05901122	(0.010823%)*
5	5	0.0010	21.84613402	21.9570277	(0.50761%)*

* Percentage decrease

In table (3.1), it can be observed that when the tangent loss is very low or 0 , the error difference between the input impedance of the simulation and calculation is higher than when the tangent loss is greater than 0.0001. This is attributed to the approximations considered in the equations. Typically, a dielectric material with a tangent loss of 0 could be considered a lossless material (input impedance of lossless coupled resonator ≈ 0 , fig 3.7), but with high dielectric permittivity, there is inherent loss in the dielectric material

even though the loss tangent is 0 as well as the loss due to the resistivity (ρ) equal 1 from fig (3.10). These losses are well accounted for in dielectric material with higher permittivity and higher tangent by using the quality factor (inverse of tangent loss) as seen in equation (3.5g). Table (3.1) validates the equations for the input impedance of a coupled resonator since the error difference between the simulation results and calculations are within acceptable limits especially for higher values tangent losses.

3.5 Group Delay of a Coupled Resonator

From the review of group delay in Chapter 2, for a coupled resonator with given input impedance as obtained in equations (3.5a-h), the group delay of a given resonator will be dependent on the dielectric permittivity of the material contained in the resonator. There is a shift in resonant frequency of a coupled resonator as a result of the value of the dielectric permittivity as shown in Fig (3.11), while a change in dielectric loss (loss tangent) for coupled resonators with sample dielectric permittivity of same real part of the dielectric permittivity impact on the height and bandwidth of the group delay plot and not the frequency as shown in Fig (3.12):

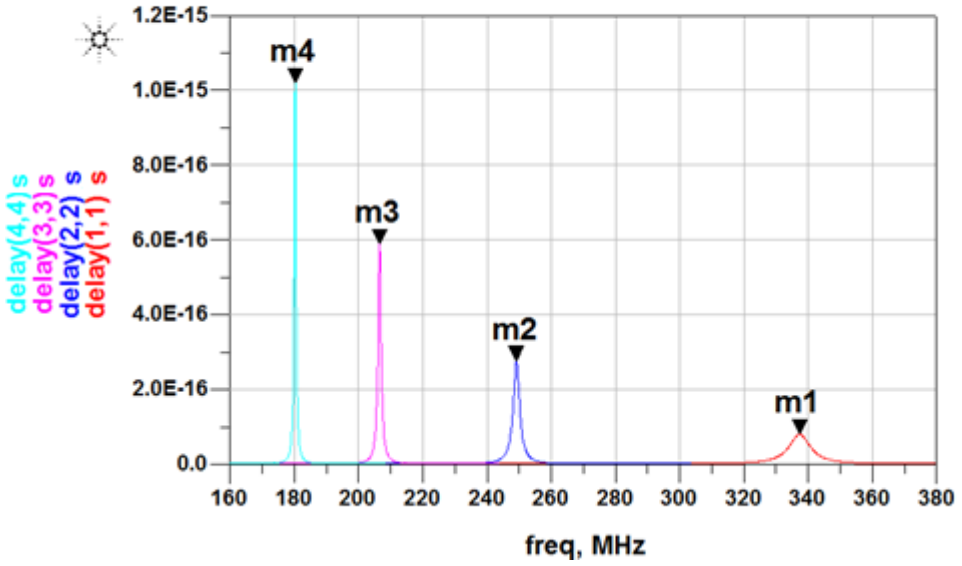

Figure 3:11: Group Delay Plot for a Coaxial Resonator measuring device for different relative dielectric permittivity (m1 (ε_r=1), m2 (ε_r=2) m3 (ε_r =3), m4 (ε_r =4)) and loss tangent is constant (tan δ =0)

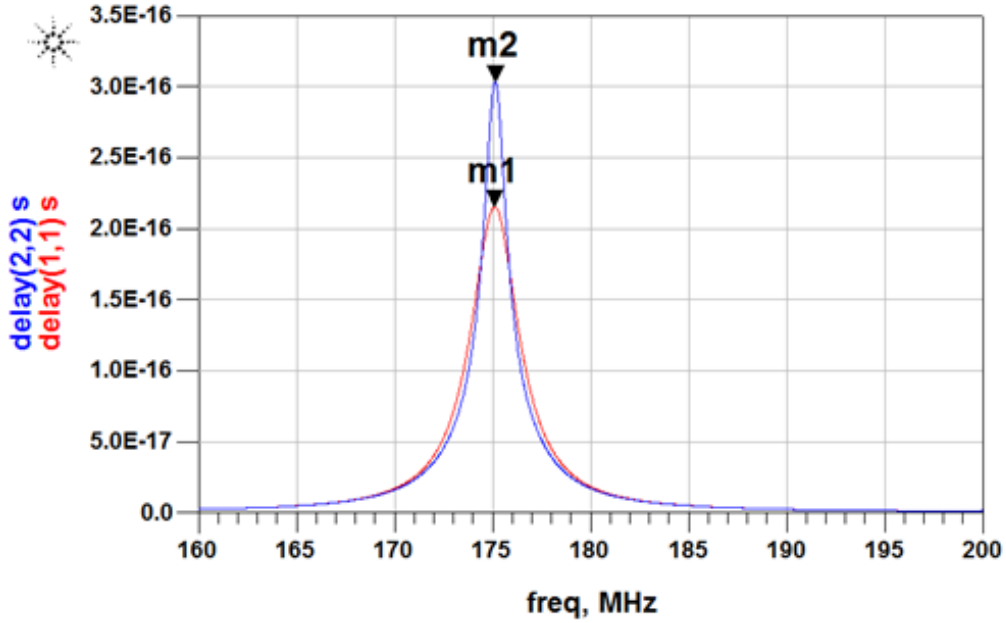

Figure 3:12: Group Delay Plot for a Coaxial Resonator measuring device for different tangent loss values (m1 (tangent loss=0), m2 (tangent loss=0.01) ε_r is constant = 4

From fig (3.12), the plot shows that the effect of loss on the group delay for a given coupled resonator can be described by the quality factor of the resonator since the difference between m1 (red) and m2 (blue) is best expressed by the quality factor of the plots (same resonant frequency but different bandwidth). In essence, for a given coupled resonator with a dielectric material, the variation of the complex permittivity of the dielectric (real and imaginary part) influences group delay plots as illustrated in Fig (3.11) and Fig (3.12)

Considering the review of the group delay theory in chapter 2 and evaluating the group delay of a coupled resonator using the input impedance obtained for coupled resonator from equations (3.5a-h), we have

Case 1: Lossless case using equation (3.5f)

$$S_{11} = \frac{Z_{in} - Z_o}{Z_{in} + Z_o} = \frac{\mathrm{j}P(\omega - \omega_o) - Z_o}{\mathrm{j}P(\omega - \omega_o) + Z_o}$$

$$\emptyset = -\arctan\left[\frac{\mathrm{P}\,(\omega - \omega_o)}{Z_o}\right] - \arctan\left[\frac{\mathrm{P}\,(\omega - \omega_o)}{Z_o}\right] = -2\arctan\left[\frac{\mathrm{P}\,(\omega - \omega_o)}{Z_o}\right]$$

$$\Gamma_d = -\frac{\delta\phi}{\delta\omega} = \frac{\delta}{\delta\omega}\left[2\arctan\left[\frac{\mathrm{P}\,(\omega - \omega_o)}{Z_o}\right]\right]$$

$$\text{Group Delay} = \frac{2P}{Z_o\left[\frac{\mathrm{P}^2(\omega - \omega_O)^2}{(Z_O)^2} + 1\right]},$$

At resonance,

$$\text{Group Delay} = \frac{2P}{Z_o} = \frac{2}{Z_o}\left[\left(\frac{l\sqrt{\varepsilon_r}}{cZ_t(B_c)^2} + \frac{Z_t l\sqrt{\varepsilon_r}}{\mathrm{c}} + \frac{1}{B_c\omega_o}\right)\right] \tag{3.6}$$

Case 2: Lossy case using equation (3.5h), we have

$$S_{11} = \frac{Z_{in} - Z_o}{Z_{in} + Z_o} = \frac{\mathrm{j}P(\omega - \omega_o) - Z_o + R}{\mathrm{j}P(\omega - \omega_o) + Z_o + R}$$

$$\emptyset = \arctan\left[\frac{P\,(\omega-\omega_o)}{R-Z_o}\right] + \arctan\left[\frac{P\,(\omega-\omega_o)}{R+Z_o}\right]$$

But Group Delay, $\Gamma_d = -\frac{\delta\phi}{\delta\omega}$

At resonance, $\Gamma_d = \frac{P}{Z_o-R} + \frac{P}{Z_o+R}$

$$\Gamma_d = \frac{2PZ_o}{{Z_o}^2 - R^2} \qquad (3.7)$$

But equation (3.6) and (3.7) can be used to evaluate the value of P. In the various equations obtained above, for a given capacitively coupled transmission line with air (empty resonator, permittivity equals 1) as the dielectric material, the coupling Susceptance, B_c can be obtained and when same coupled resonator is filled with a dielectric material while maintaining the gap (coupling Susceptance, B_c), this alters the characteristic impedance, Z_t, of the resonator from which the relative permittivity, ε_r, of the material can be extracted. Equation (3.7) is used to obtain the characteristic impedance, Z_t, when the resonator contain the dielectric material to be tested, this is in turn used to extract the relative dielectric permittivity value, $\boldsymbol{\varepsilon}_r$.

The dielectric material is contained inside coupled coaxial resonator between the inner and outer conductors. The filling of the dielectric material of unknown permittivity values replaces air as the permittivity in the resonator. Thus, using equation (3.7), the relative dielectric permittivity of the material can be obtained.

3.6 Determining the Quality Factor & Tangent Loss of Coupled Resonator

The losses associated with a coupled resonator can be contributed by the metal wall conductivity, the dielectric contained in the resonator as well as coupling to the resonator and these can be quantified by the quality factor of the resonator.

In chapter 2, the relationship between external quality factor and group delay expressed in equation (2.23b) holds for a lossless coupled resonator. (Ness, 1998) Also expressed the group delay relationship for a coupled resonator with loss as:

$$\frac{Q_E}{1-\left(\frac{Q_E}{Q_U}\right)^2} = \frac{\omega_o \Gamma_d(w)}{4} \tag{3.8}$$

Where $\frac{Q_E}{Q_U}$ = K = Coefficient of coupling is the ratio

From substitution, using equation (2.7), loaded quality factor can be expressed as:

$$Q_L = \frac{(K-1)}{K}\frac{\omega_o \Gamma_d(\omega)}{4} \tag{3.9}$$

Also, K can be expressed in terms of the magnitude of the reflection coefficient as

According to (Ness, 1998), $K = \frac{Q_u}{Q_E} = \frac{1+|S_{11}|}{1-|S_{11}|}$ (3.10)

Therefore, equation (3.9) can be rewritten as

$$Q_L = \frac{2|S_{11}|}{1+|S_{11}|}\frac{\omega_o \Gamma_d(\omega)}{4} \tag{3.11}$$

The unloaded quality factor is obtained from equation (3.11). This value is the quality factor of the uncoupled resonator which is dependent on the losses associated with the dielectric material contained in the resonator as well as the losses due to conductivity of

the metal walls. For a coaxial with certain conductivity, quality factor due to metallic conductivity, Q_c ,is given by equation (2.11). Therefore, using equation (3.12) below, the loss tangent of a certain dielectric material contained in the coupled coaxial resonator can evaluated.

$$Q_u = \left(\frac{1}{Q_c} + \frac{1}{Q_d}\right)^{-1} \qquad (3.12)$$

Where Q_d =Quality factor due to the dielectric losses $= \frac{1}{Loss\ Tangent}$

Q_c= Quality factor due to the conductor losses.

Chapter 4: Design & Analysis of an Over-Coupled Coaxial Resonator

4.1 Introduction

The design parameters and specifications were obtained from model analysis using electromagnetic simulations. This helps to understand how best the resonator can be coupled to obtain the coupling capacitance, when the resonator is empty, and the dielectric permittivity values when the resonator is filled with a dielectric material.

4.2 Design of an Over-Coupled Coaxial Resonator

The design specifications for an over-coupled coaxial resonator are based on the equations and concepts established in chapter 3. In choosing the length of the resonator given by the length of the inner conductor, the outer conductor is longer than the inner conductor from the upper end of the resonator and with the coupling mechanism sealing the top, radiation loss is minimised. However, this section of the coaxial resonator, between the top of the inner conductor and the cap of the coupling mechanism of the resonator contains the gap providing the coupling capacitance, C. As shown in Fig (4.1)

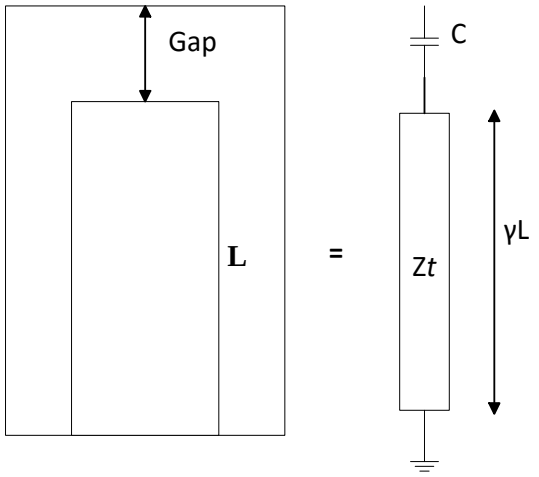

Figure 3:13: Model of a Gap-coupled coaxial resonator

Z_t is the characteristic impedance which is dependent on the dimensions of the coaxial resonator (the inner and outer diameter of the conductor) and the dielectric material between the inner and outer conductor.

From equation (3.5a) and fig (3.7), it can be observed that at resonance, the input impedance is approximately equal to 0 (for a lossless case) and minimum at resonance for a lossy case. For a quarter wavelength resonator, using equation (4.1), the value of the capacitance, C, will be equal to zero at resonance. This means that the gap distance will be infinite to provide zero capacitance assuming no other capacitance is introduced due to fringe effects of the electromagnetic fields. Figure (4.2) shows how capacitance varies with gap distance for a given coaxial resonator

$$C = \frac{1}{\omega Z_t \tan\gamma \mathrm{l}} \qquad (4.1)$$

Therefore, the length of the coaxial resonator should be less than a quarter wavelength of the operating frequency, from equation (4.1), so as to have a reasonable gap distance and in turn a capacitance value to provide the necessary coupling.

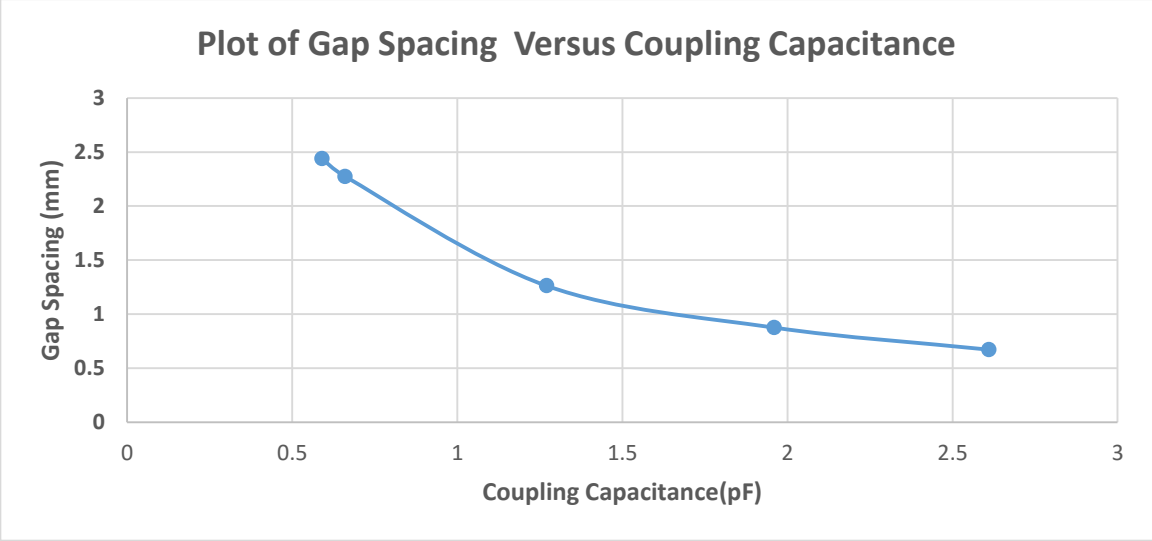

Figure 3:14: Simulation Plot of Gap Distance versus Coupling Capacitance of a Gap-Coupled Coaxial Resonator

From the plot in figure (4.2), it is observed that the smaller the gap distance, the higher the coupling capacitance.

With the ability to vary the gap distance, the coupled coaxial resonator measuring device could be employed for samples of different degree of losses provided the coupling capacitance from the gap is high enough to make the resonator over-coupled. Under-coupling as a result of low coupling capacitance with respect to the dielectric permittivity values of the dielectric material results in negative group delay which is not desirable for this study.

The ratio of the diameter of the outer conductor and the inner conductor affects the characteristic impedance,Z_t, but the values of these diameters to provide the desired ratio should be chosen so as to provide the necessary coupling capacitance. This is because, two resonators with the same gap distance but different respective diameters for both the inner and the outer conductors yield separate coupling capacitance. As a result, the gap capacitance is provided by the diameter of the inner conductor of the resonator and that of the coupling mechanism.

Having the desired resonator dimensions and coupling capacitance are not the only considerations required to arrive at the specifications for a given coupled resonator design. Since the characteristic impedance changes with the dielectric material, the resonant frequencies for an empty gap-coupled coaxial resonator and that filled with a dielectric material are different (from fig (3.11)). Capacitance varies with frequency, so it is desirable that for a chosen design specification, the capacitance should be constant over the frequency range which measurement will be carried out. Figure (4.3) shows how capacitance is constant for different gap spacing for a design specification given in table (4.1).

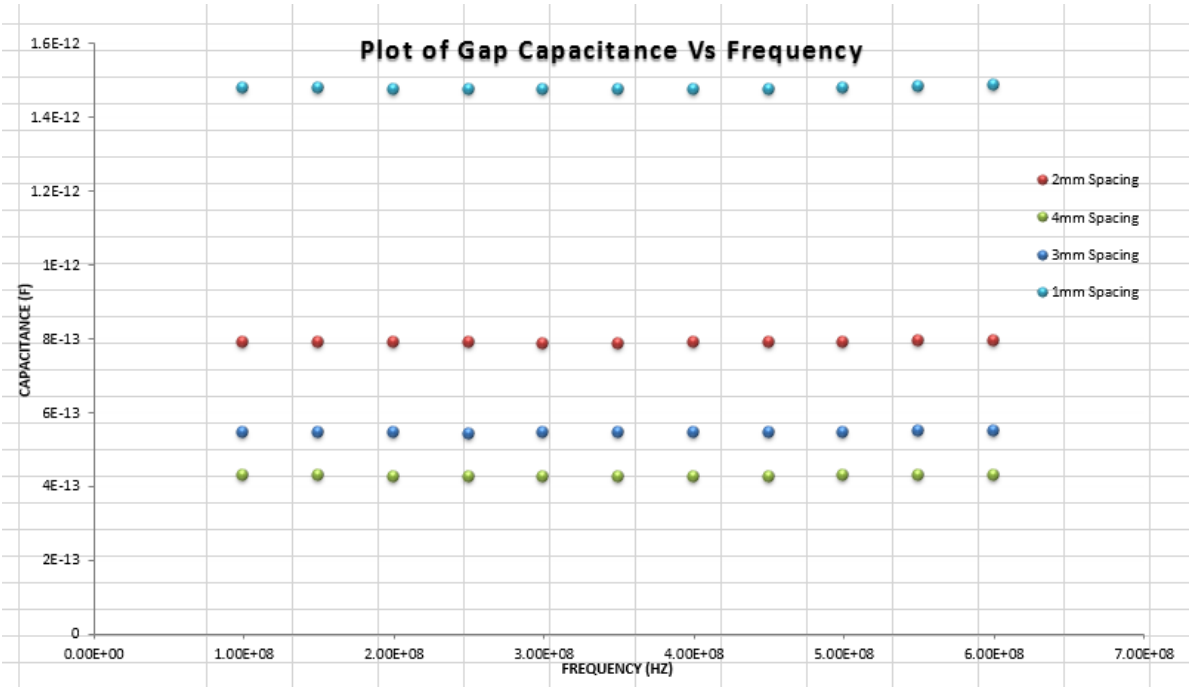

Figure 3:15: Plot of Gap Capacitance versus Frequency

4.2.1 Design Specifications

The specifications for the resonator were chosen such that the operating frequency for the uncoupled resonator is 350MHz. The length of the resonator is less than quarter wavelength of the operating frequency so as to accommodate the effect of the coupling capacitance.

The inner and outer diameter values were chosen such that they give a capacitance large enough to maintain the desirably over-coupling for certain range of dielectric measurements.

A summary of the design specifications used for this study is given in table 4.1

Table 3.2: Design Specifications

Parameters	**Values**
Maximum Length of resonator	189.2mm
Inner Diameter of Resonator , $Ø_1$	12.7mm
Outer Diameter of Resonator, $Ø_2$	31.75mm

The maximum length from table (4.1) is the length of the inner conductor

4.2.2 Design Model

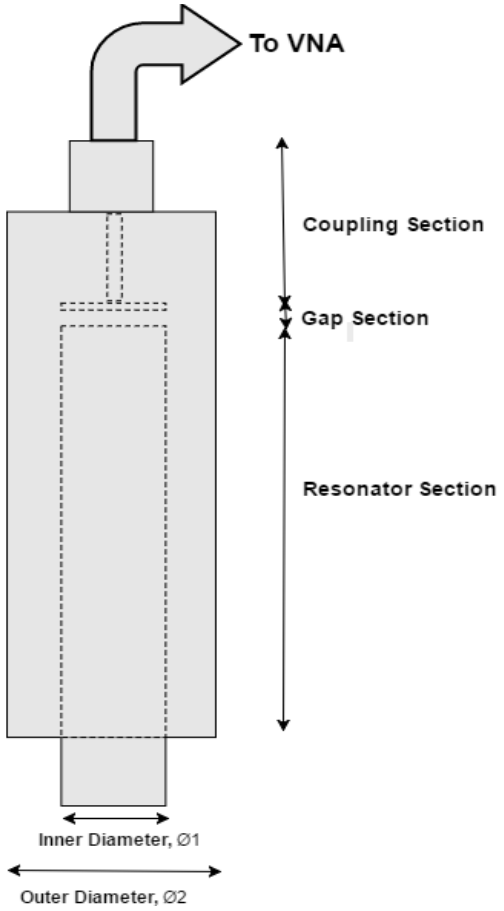

Figure 3:16: Model Design of a coupled coaxial rsonator measuring device

The model design consists of the coupling section connected to a vector network analyser (VNA) and the resonator section which contains the dielectric material to be measured. The coupling section has a plate placed on the bottom end of the inner conductor of a 50Ohm N-type coaxial connector (Fig 4.5), this forms a parallel plate with the top end of the resonator inner conductor, thereby providing a coupling capacitance as a result of the gap formed by the plates.

Figure 3:17: 50 Ohm RF Connector, N-Type Straight Solder Plug (Amphenol RF, 2017)

4.3 Design Analysis

To better understand the study, electromagnetic simulation applications (ADS and HFSS) were used to simulate the behaviour of a gap-coupled coaxial resonator. This involves determining the coupling capacitance when the coaxial resonator is empty which is then used in evaluating the dielectric permittivity of a given sample material as well as the

unloaded quality factor of the coupled resonator device filled with the sample provided the capacitance is constant over the new resonant frequency when the sample is introduced (shown in Figure 4.3).

4.3.1 Simulations Using Gap-Coupled Coaxial Resonator

Systemic procedures were taken by ensuring that the gap-coupled resonator was initially modelled as a lossless resonator, this is done by using a perfectly electric conductor (PEC) as the resonator thereby reducing the complexity of the set-up before advancing to cases where the resonator is lossy. For lossy case, a coaxial resonator with finite conductivity, (Aluminum), was used. This is followed by analysis involving losses from the dielectric sample.

Results from both software (ADS-circuit simulator and HFSS- full electromagnetic wave simulator) are compared and appropriately optimised when necessary so as to arrive at the parameters for the measurement in the physical design of the gap-coupled resonator.

In HFSS simulation, steps are taken to ensure accuracy of simulation of results aside repetition of a simulation process. Depending on the 3D structure, HFSS creates meshes using the set criteria for convergence of the simulation. The finer the meshes, the more accurate the simulation becomes. Complex 3D structures require thousands of meshes to ensure electromagnetic analysis of the structure is carried out. However, the gap-coupled coaxial resonator design is a relative less complex structure with the design settings.

From the specification of the coaxial resonator design, the set criteria for the convergence are as follows:

Maximum number of passes: 20

Maximum Delta S = 0.02

The Solution Frequency is dependent on the resonant frequency of the resonator which varies when the resonator is empty and when a dielectric sample is introduced. Because this frequency is not known initially for a given sample, the meshing is first done at a relatively higher solution frequency before re-meshing at the obtained resonant frequency, this ensured the system accurately convergences at the desired resonant frequency.

Convergence is achieved when HFSS compares the s-parameters results after each adaptive passes and no noticeable change between the current mesh and that of the previous mesh from the defined values before the simulation, in this case Delta S equals 0.02.

In the simulation of the design model using HFSS, a reference plane is defined so as to de-embed the coupling section of the model. This way, the analysis is focused on the resonator section. This is done by defining the distance from the top end of the N-type connector to the top plate just before the gap of the model (as shown from the arrow in Fig 4.6). In physical test environment using a vector network analyser (VNA), this process is realised via calibration of the VNA. This ensures accuracy of the results because it excludes the effect of cables and connector between the VNA and measuring test device.

The coupling capacitance evaluated from using equation (3.7), in this case, the relative permittivity, $\boldsymbol{\varepsilon}_r$, equals 1 since the resonator is empty can be obtained using the simulation results from Figure (4.7) - Figure (4.9).

From the group delay plot, (Ness, 1998) has mentioned that for a plot of bandwidth greater than 1%, the plot is not symmetrical about the resonant frequency. To accurately locate the resonant frequency, the plot of the input impedance versus frequency or Z parameter

plot (Z_{11}) is used as shown in Figure (4.7). At this frequency, the input impedance is minimum, and the concept of which the design equations and analysis were based on the fact that input impedance is minimum at resonance (section 3.4.3). Therefore, locating the resonance frequency from plot of the input impedance is necessary. The group delay and S_{11} information obtained from the plots at this frequency are used to compute the coupling capacitance.

Figure 3:18 : HFSS Design Model of a Coupled Coaxial Resonator Measuring device

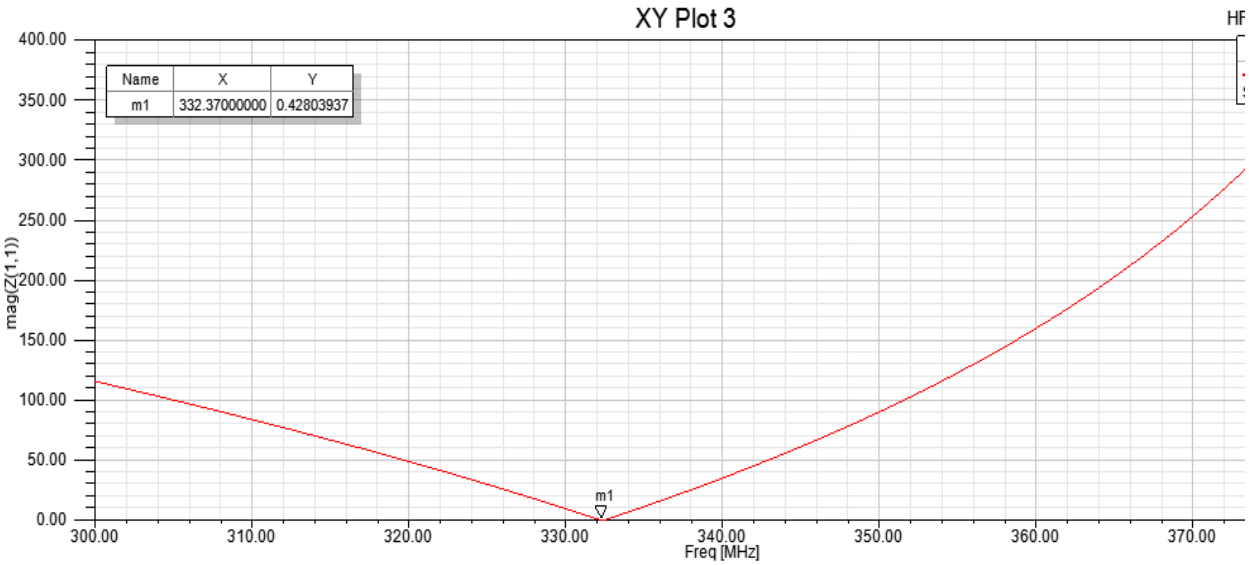

Figure 3:19: HFSS Design Model of a Coupled Coaxial Resonator Measuring device

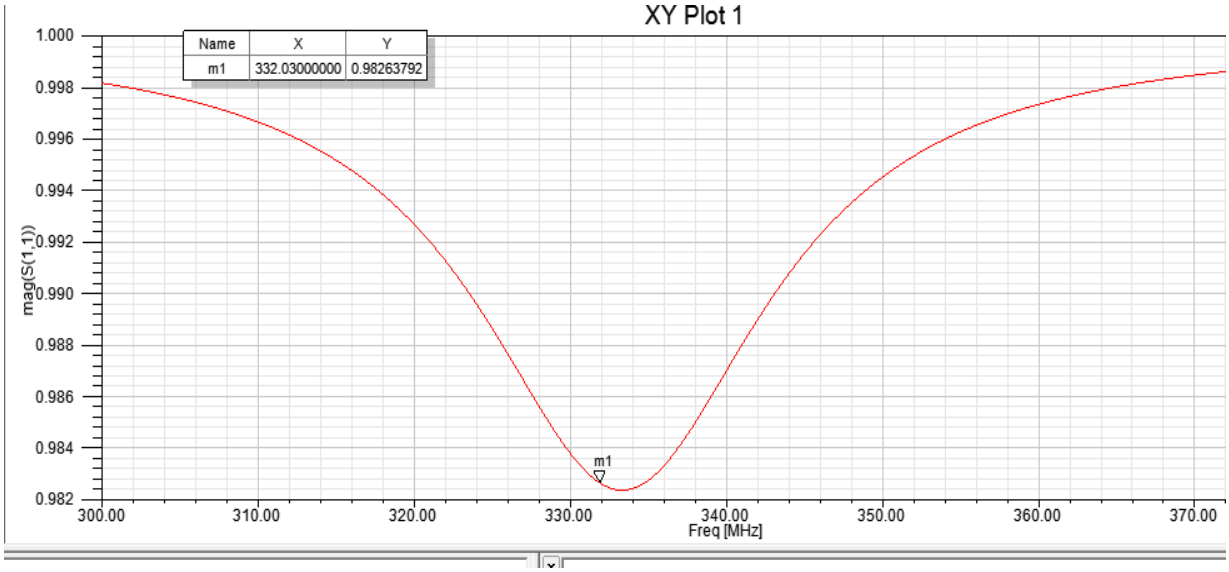

Figure 3:20 : HFSS Plot of Magnitude of S11 versus Frequency (MHz)

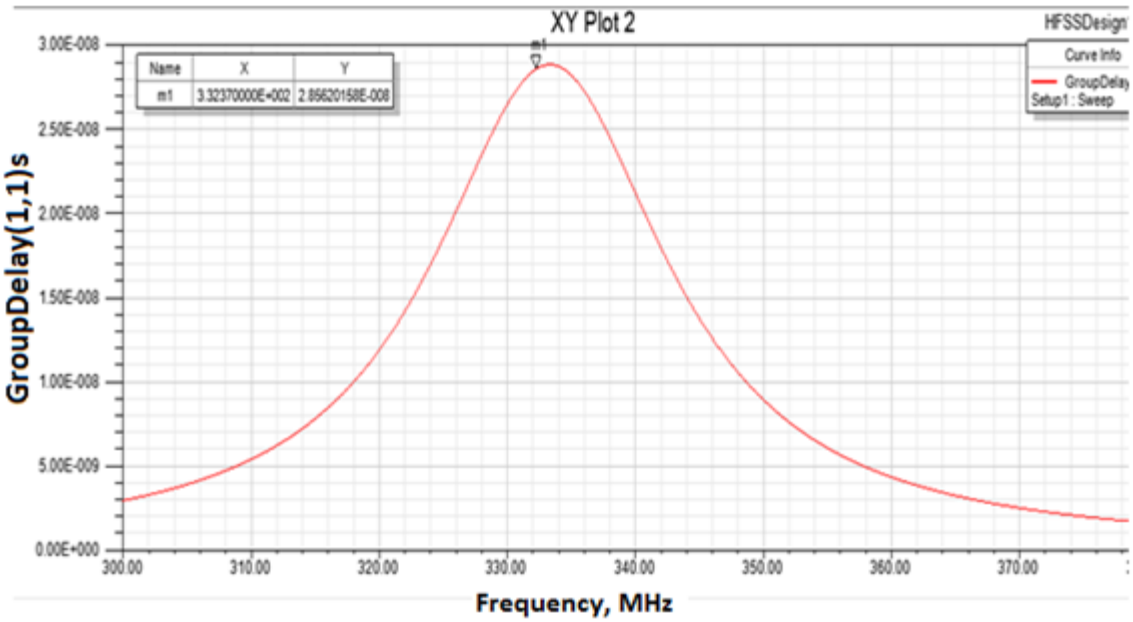

Figure 3:21 : HFSS Plot of Group Delay of reflection coefficient versus Frequency (MHz)

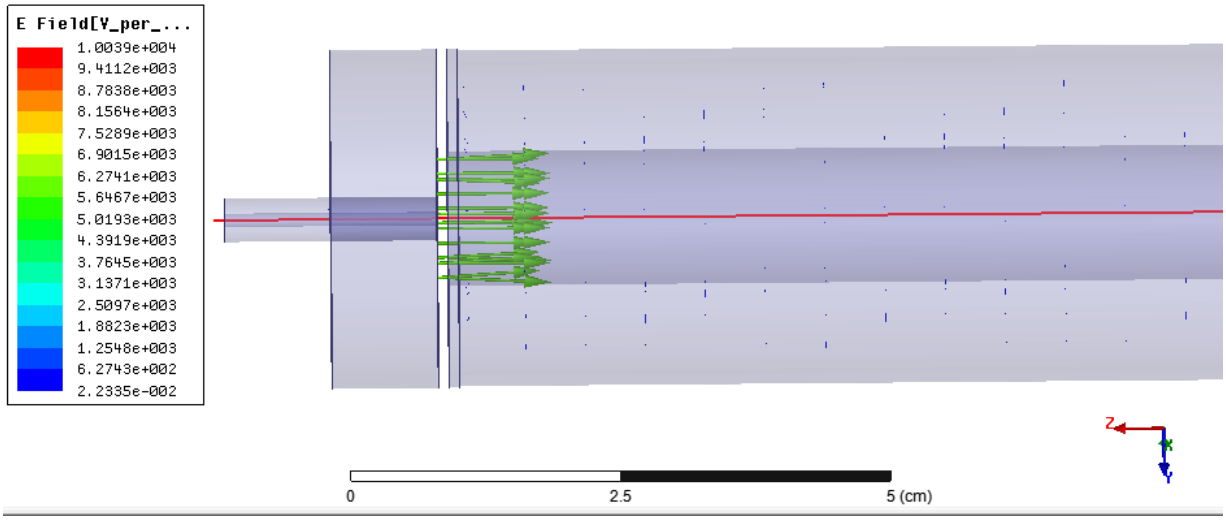

Figure 3:22: Electric Field plot of the empty resonator measuring cell.

Table 3.3: Capacitance and Quality factor of empty coupled resonator model

Coupling Capacitance (F)	2.14048257e-12
Quality Factor	1702.7109073

The table above is the computation of coupling capacitance and the unloaded quality factor with gap spacing of 0.59mm when resonator is empty using the information fig (4.7) – fig (4.9).

4.3.2 Estimating the Dielectric Permittivity of Samples Using Loaded Gap-Coupled Coaxial Resonator Measuring Device

Filling the measuring device (the resonator section) with dielectric sample and maintaining the gap between the coupling section and resonator section (using the coupling capacitance obtained in Table (4.2)), the relative dielectric permittivity value can be obtained using equation (3.7).

From Figure (4.12), it is observed that there are electric fringe fields in the gap section of the measuring device when the dielectric sample fills the resonator section. This affects the accuracy of the estimated dielectric permittivity ($\boldsymbol{\varepsilon}$) because the gap capacitance is affected by these fringe fields. To minimise the errors caused by electric fringe fields, few millimeters of clearance is allowed. The analysis in table (4.3) shows that allowing for 1mm clearance when filling the resonator section with a given dielectric increases the accuracy of measurement and also reduces the electric fringe fields in the gap section (fig 4.13)

Table 3.4: Analysis of dielectric permittivity values for an over-coupled resonator measuring device.

Clearance	Capacitance Empty (pF)	Sample Permittivity ,2.1 (% Difference in permittivity) Loss 0.0002	Sample Permittivity, 3.5 (% Difference in permittivity) Loss 0.0018	Sample Permittivity, 4.5 (% Difference in permittivity) Loss 0.002
0mm	2.14048257	2.051953 (2.287945%) 0.0002216	3.340339282478 (4.5617347%) 0.002455	4.28419366938 (4.795696%) 0.004124
1mm		2.0930801839 (0.329515%) 0.00020289	3.493572472342 (0.1836436%) 0.002012	4.35227105429 (3.282865%) 0.002789

From table 4.3, it can be observed that filling up the resonator section (0mm clearance) provided permittivity values with higher percentage errors but allowing a 1mm clearance between the top end of the resonator and the dielectric provides a better permittivity values.

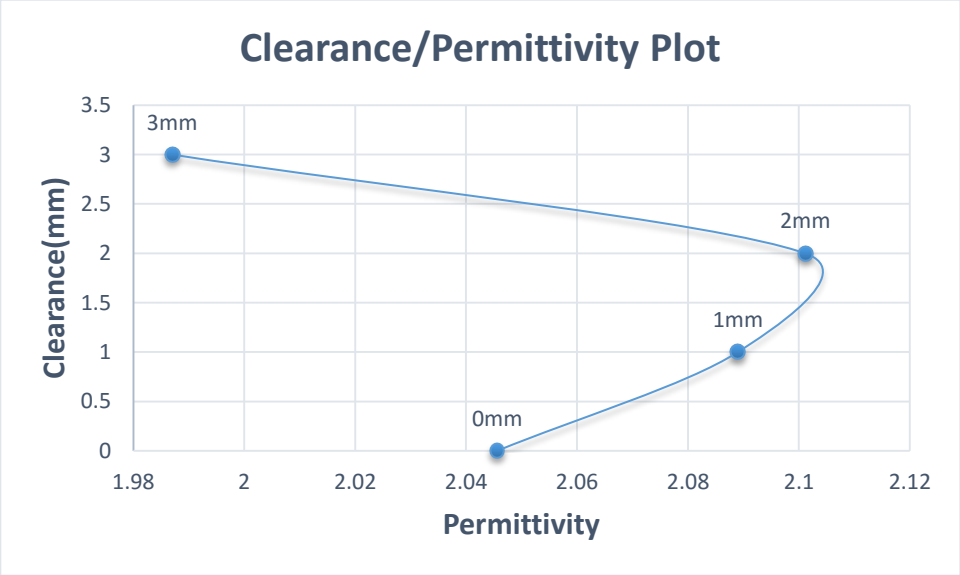

Figure 3:23: Plot of Clearance vs Permittivity

Fig 4.11 shows how the clearance improves the percentage error for a resonator containing a sample permittivity of 2.1. It can be observed from the plot that at clearance between 1.5mm and 2 mm gives the optimum value of the permittivity.

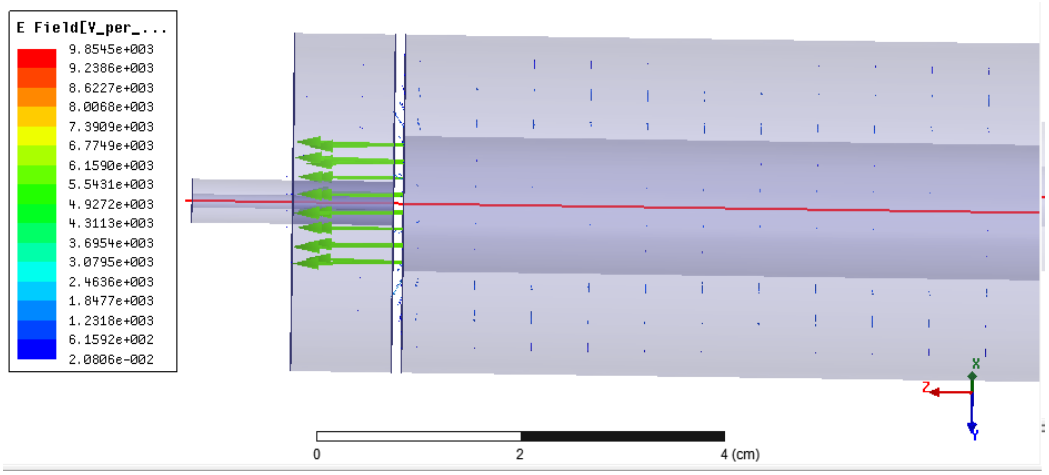

Figure 3:24: HFSS Electric field plot showing electric fringe fields in the gap section when measuring device is filled with dielectric sample

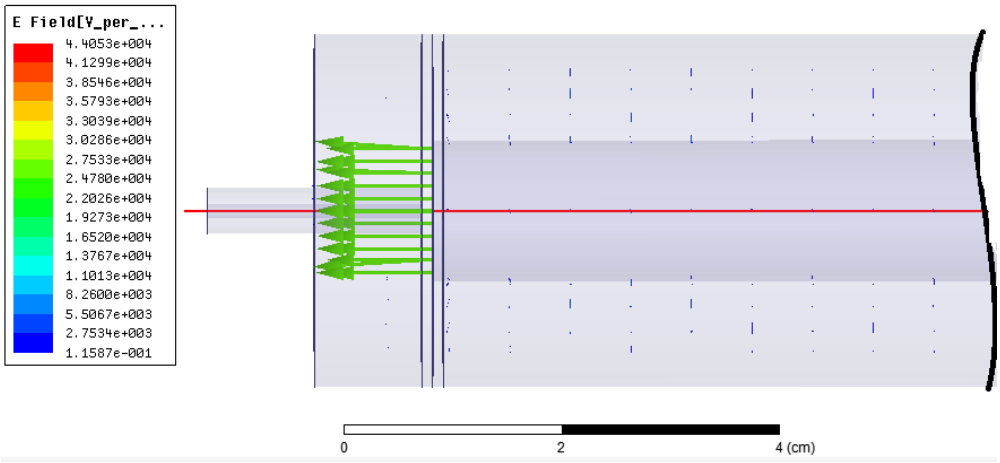

Figure 3:25: HFSS Electric field plot showing reduced electric fringe fields

Chapter 4 **: Fabrication, Testing & Results**

5.1 Introduction

This chapter focuses on testing using the fabricated gap-coupled coaxial resonator designed using parameters developed in chapter 4. The resonator is tested when it is empty to obtain the coupling capacitances, and the coupling capacitance values obtained for various gap distances are compared with the simulation values. This is required to validate the results from fabricated resonator with the simulation results. Thereafter, sample of known electrical properties (Teflon) is tested to validate the proposed method.

5.2 Experimental Setup & Test Procedure

The experimental setup consist of the fabricated resonator designed using the parameters in table (4.1). Maximum length of the resonator is the length of the inner conductor that will provide zero gap spacing between the top end of the inner conductor and the plate placed on the coupling mechanism connecting to the VNA. Gap spacing is used to obtain coupling capacitance by reducing the length of the conductor (via tuning the inner conductor).

The fabricated resonator has the inner and outer conductor made from aluminum with conductivity of 35.46e6 S. The relatively good conductivity of aluminum makes it a preferred choice for this application because this will minimise the conductor losses. The connector with characteristic impedance of 50 Ohm (fig 4.5) is used in the coupling mechanism. This will minimise the reflections caused as a result of impedance mismatch at the input when the device is connected to the Vector Network Analyser (VNA)

Before connecting the fabricated resonator to the VNA, a full one-port calibration is first performed on the VNA. This allows for error correction caused by imperfections in

measurement that could result from the effect of cables and adapters connected to the gap-coupled resonator. The test set up is shown in fig (5.1) and Fig (5.2) with the VNA connected to a computer display.

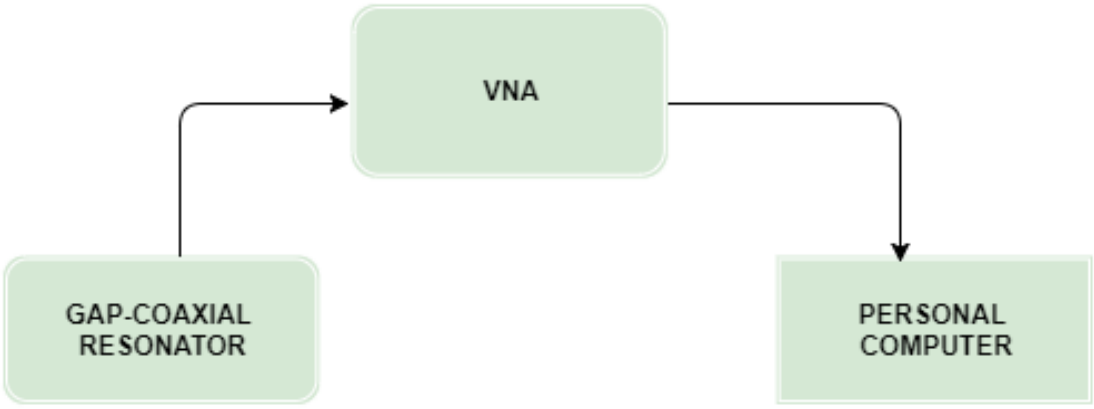

Figure 4:1: Block diagram of Experimental Set-up

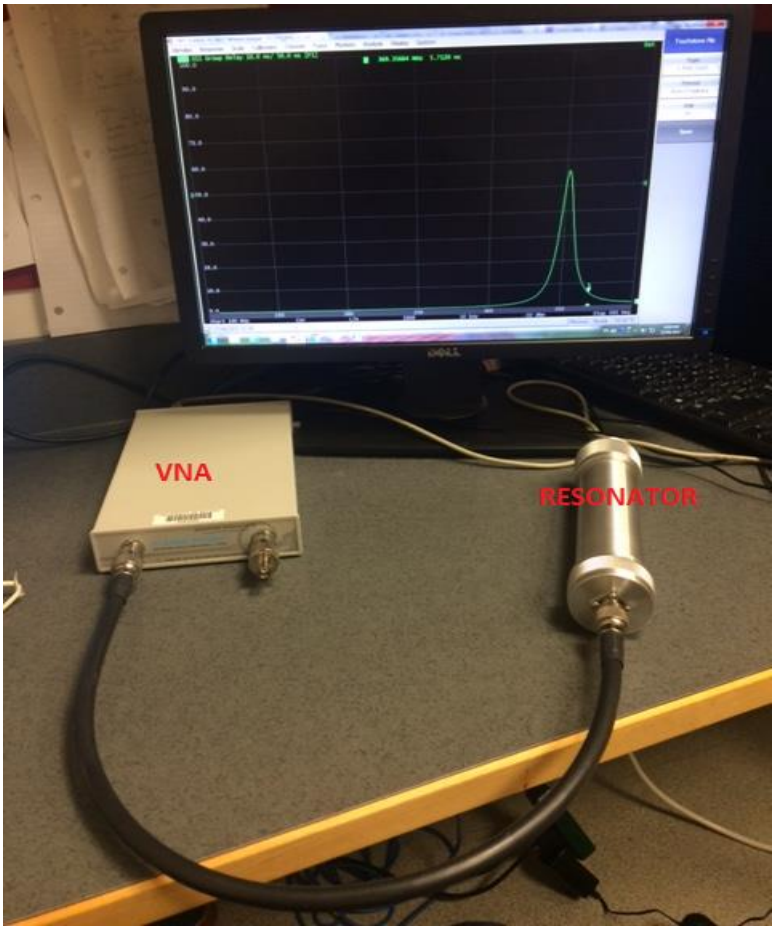

Figure 4:2: Test Setup

A summary of the test procedure is given below:

a) The VNA is calibrated for Full 1-port Calibration with frequency limits of 100MHz – 400MHz.

b) The empty resonator is connected to the VNA with the desired gap spacing to make the resonator over-coupled.

c) The group delay values and the input reflection coefficient are measured for the empty resonator and their values obtained at resonant frequency.

d) The values of the input reflection coefficient, the group delay and the resonant frequency obtained above are applied to equation (3.7) in order to determine the coupling capacitance, C.

e) Maintaining the resonator gap spacing, the dielectric material sample is introduced into the resonator and measurements of the group delay as well as the input reflection coefficient are obtained at resonant frequency when the resonator is filled with the dielectric sample.

f) Repeating step (c), the evaluated value of the coupling capacitance, C, the values group delay, input reflection coefficient and the resonant frequency are applied to equation (3.7) to determine the relative permittivity, $\boldsymbol{\varepsilon}_r$, of the dielectric material.

g) Also, to determine the loss tangent, tan δ, the values of group delay, input reflection coefficient and the resonant frequency are applied to equation (3.11). This will give the loaded quality factor, Q_L , of the coupled resonator. The relationship between the unloaded quality factor, the loaded quality factor and the external quality factor given by equation (2.7) will allow unloaded quality factor to be evaluated.

h) The unloaded quality factor is composed of the quality factor due to the conductivity of the metallic walls of the resonator, Q_c and the losses due to the dielectric. The fabricated resonator was made using aluminum of conductivity 35.46e6S. The loss tangent of the dielectric material is evaluated from the reciprocal of the quality factor due to the dielectric loss, $Q_{d.}$ from equation (2.10).

5.3 Coupling Capacitance

For different gap spacing, the coupling capacitance is obtained for the fabricated resonator. Fig (5.3) shows a plot of coupling capacitance versus gap spacing. This is compared to the

plot obtained from the simulations using the electromagnetic simulation software (HFSS) in Fig (4.2).

The plot in fig (5.3) also confirmed that the smaller the gap spacing, the higher the coupling capacitance. Therefore, to achieve stronger coupling small gap spacing is required, and this is also desirable for some dielectric material with relatively high dielectric permittivity and loss tangent values because higher coupling capacitance is required for the resonator to remain over-coupled.

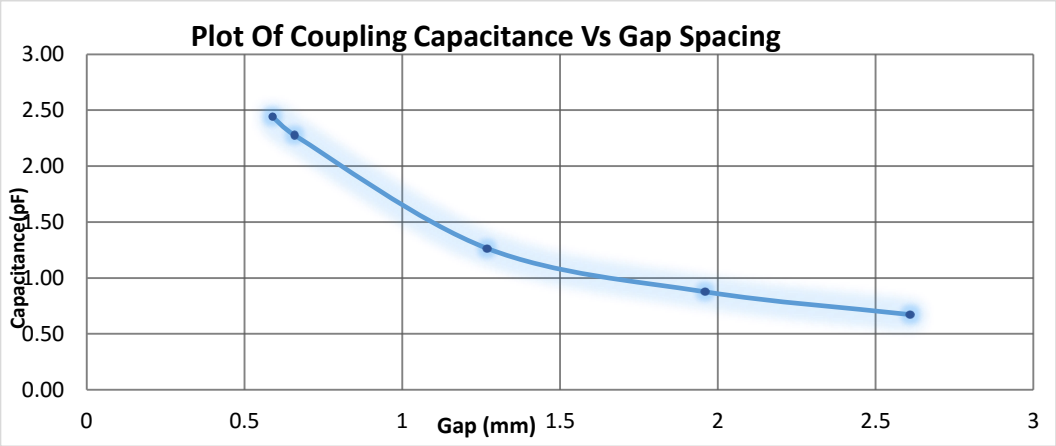

Figure 4:3: Plot of coupling capacitance vs. gap spacing for the fabricated Resonator

The group delay plot from the simulation results using HFSS is compared to the group delay measurement from the fabricated resonator test set up. This is shown is fig (5.4). This plot is obtained for a gap spacing of 0.66mm. It can be observed that the two plots from both the simulation and the fabricated resonator closely align. The slight difference between the two plots (at the peak of the plot) can be attributed to measurements inaccuracies arising from the cables used in the fabricated resonator and the reference plane from the calibration of the VNA. However, this has minimal effect in the result when each plot is independently used to extract the dielectric constant of material.

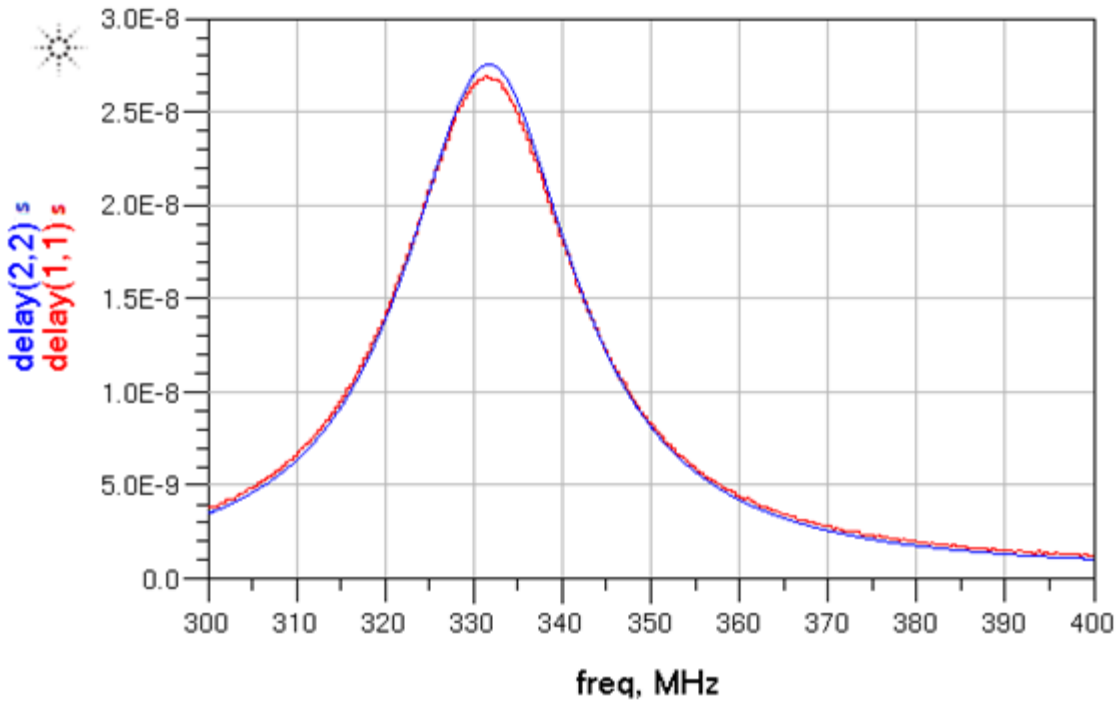

Figure 4:4: Plot of Group Delay from HFSS Simulation (Blue) and Group Delay plot from fabricated resonator (Red) when the resonator is empty

The various capacitance values for different gap spacing when the fabricated resonator is empty are shown in Table (5.1):

Table 4.1: Gap Spacing & Coupling capacitance (Empty Resonator)

Gap Spacing (mm)	Coupling Capacitance(pF)
0.59	2.44012
0.66	2.27451
1.27	1.26308
1.96	0.875972
2.61	0.6720656

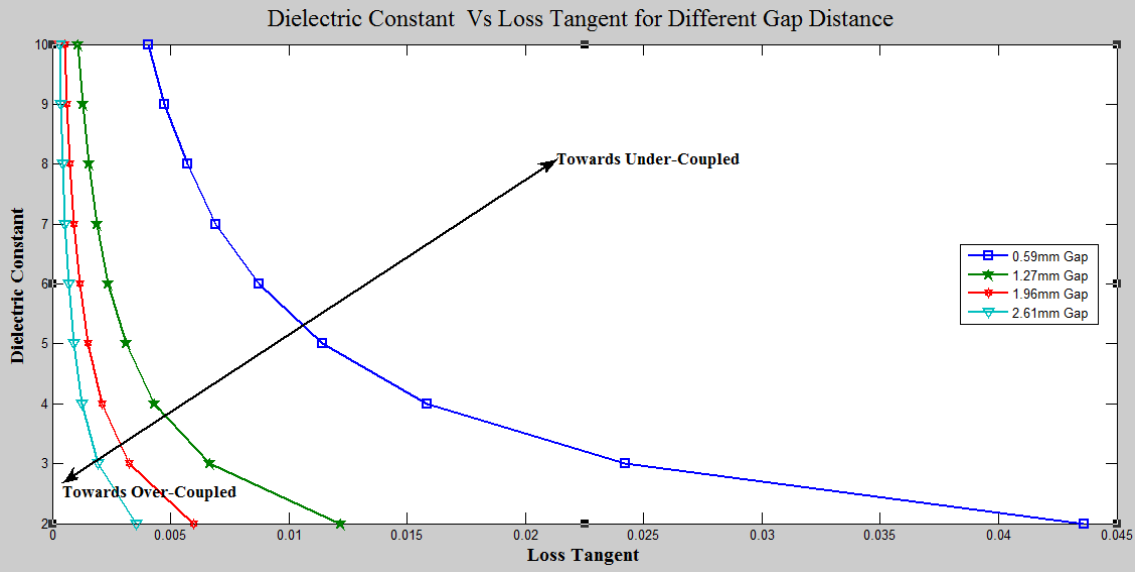

Figure 4:5: Plot of Dielectric constant and loss tangent that shows the range of values the fabricated resonator can operate

Fig (5.5) shows the limits to which the fabricated resonator can operate in an over-coupled state when different materials with varying permittivity values and loss tangent are measured. It can be observed from the plot that for each curve represented by the gap spacing/coupling capacitance, the resonator operates from over-coupled state (below the curve, for low permittivity values) to critical state at a certain permittivity value since coupling capacitance is constant. At higher permittivity values (above curve), the resonator is under-coupled. Therefore, the fabricated resonator cannot be used for values of dielectric materials that will drive the resonator to the under-coupled state using the proposed group delay method if the maximum coupling (minimum gap spacing) that will keep the resonator over-coupled is attained.

Analysing Fig (5.5) further, certain points are analysed using the maximum coupling from the figure when the gap spacing is 0.59mm (coupling capacitance of 2.44012pF) as seen in Fig (5.6) below:

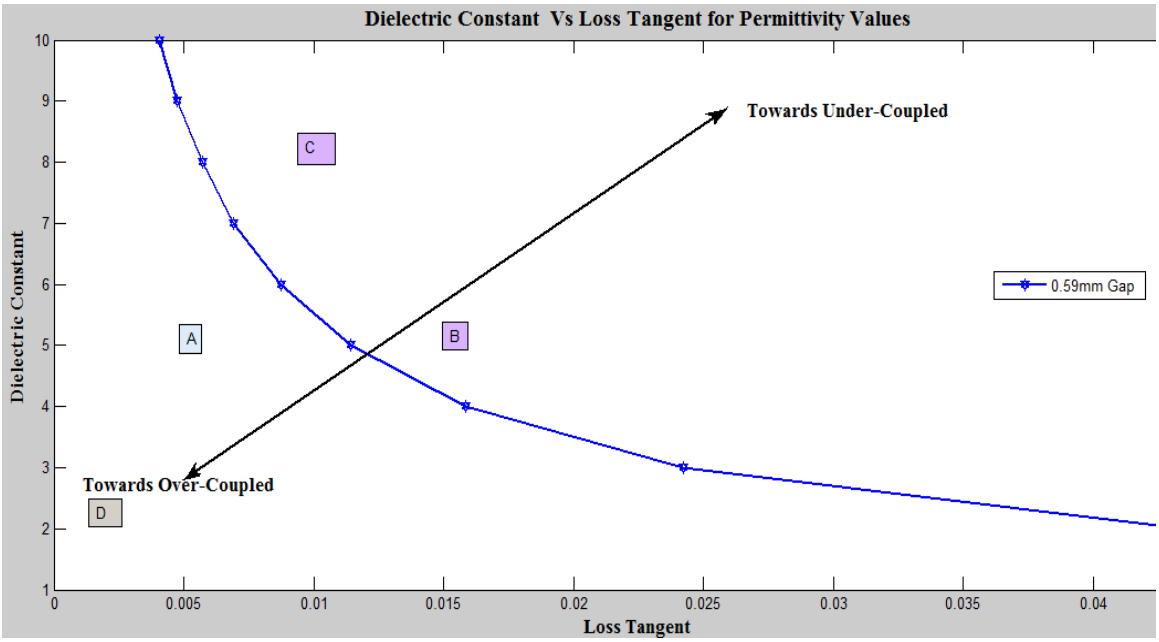

Figure 4:6: Examples of Dielectric Permittivity values

From Fig (5.6), sample points at A (Dielectric constant 5, loss tangent 0.005) and D (Dielectric constant 2.1, loss tangent 0.00015) below the curve, towards the over-coupled direction, can be easily measured using the fabricated resonator with a gap coupling of 0.59mm. For sample points at B (Dielectric constant 5, loss tangent 0.00015) and C (Dielectric constant 8, loss tangent 0.01) above the curve, towards the under-coupled direction cannot be measured if the proposed group delay method is used in determining their electrical properties.

5.4 Testing & Results

The values of the coupling capacitance obtained in fig (5.3) were evaluated when the coaxial resonator was empty. Using same gap spacing, in essence maintaining the coupling capacitance, material under test (MUT) of known electrical properties, Teflon, was tested. It was introduced into the resonator to measure its properties for a gap spacing of 0.59mm

and 1.27mm. The group delay plot shown in fig (5.4) and the reflection coefficient (S_{11}) plot in fig (5.5) were obtained. At resonance frequency, the values of the group delay information and the reflection coefficient are used to compute the dielectric permittivity value of Teflon using equation (3.7). The value of the resonant frequency changes from 327.05MHz when the resonator is empty to 257.58MHz for a gap spacing of 0.59mm as seen in Fig (5.7).This change in frequency is caused by the value of the relative dielectric permittivity, $\boldsymbol{\varepsilon_r}$

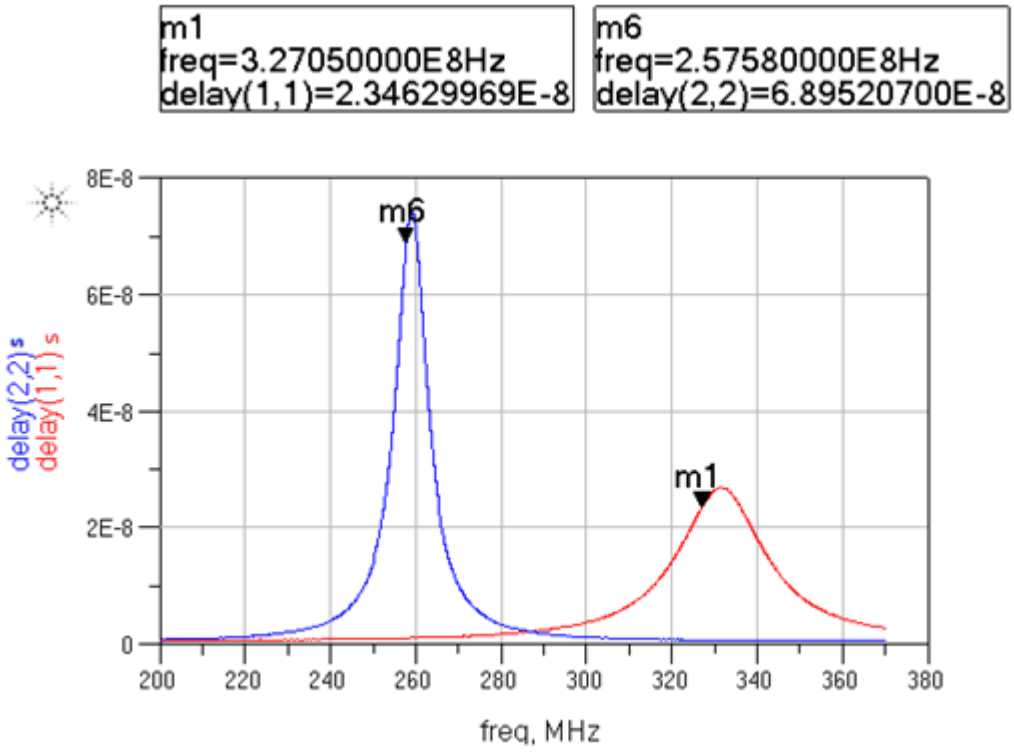

Figure 4:7: Plot of Group Delay versus Frequency when fabricated resonator empty (Red) and filled with Dielectric, Teflon, (Blue) when coupling gap is 0.59mm

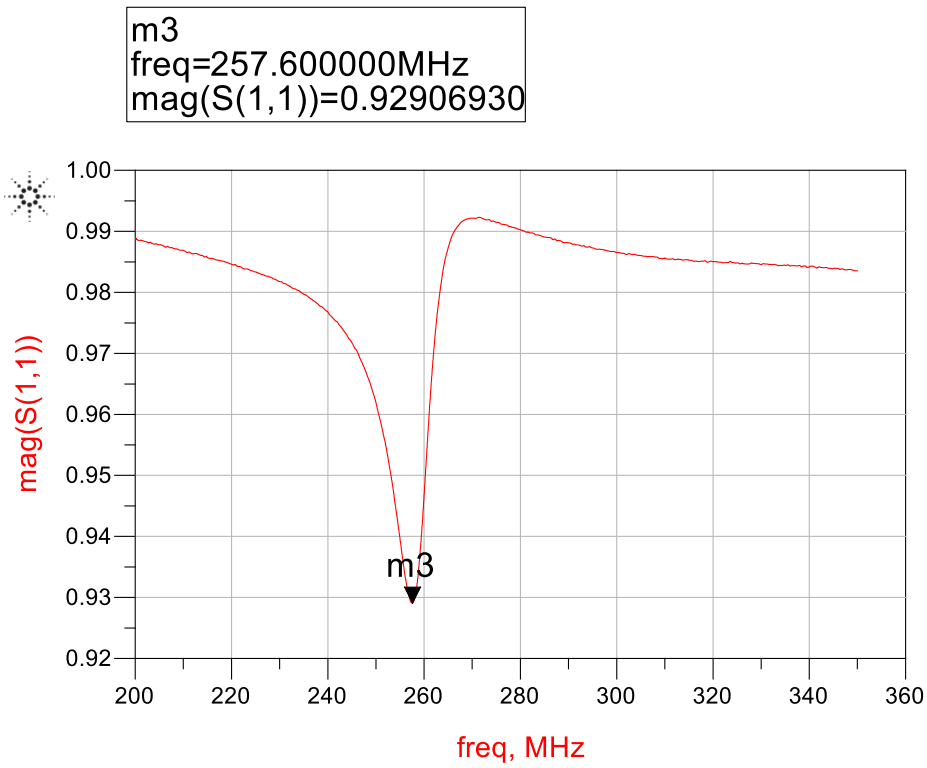

Figure 4:8: Plot of S11 versus Frequency when Resonator is filled with Dielectric (Teflon) when coupling gap is 0.59mm

With the value of the coupling capacitance (see appendices for procedure of calculation/evaluation. Matlab was used to reduce error from complexity of the equation 3.7), the group delay at resonant frequency and the input reflection coefficient, the relative permittivity values are obtained as seen in table (5.2).

Table 4.2: Results measurement of the dielectric permittivity of Teflon

Gap Spacing (mm)	Measured Relative Dielectric Permittivity	Loss tangent
0.59	2.0903365	0.00018828
1.27	2.08509314	0.00013493

The dielectric permittivity of materials tends to vary with temperature and frequency. However, Teflon has a fairly constant dielectric permittivity values at different temperature and frequency, with dielectric constant of 2.0-2.1 and loss tangent of 0.00015-0.0004 (Microwave101, 2017) . From the datasheet of the Teflon material used in this experiment (see Appendices 1), the dielectric constant and loss tangent values were measured at frequency of 50-109Hz to be 2.1 and less than 0.0002 respectively.

The results in table (5.2), fall within acceptable limits for the values of the dielectric permittivity of Teflon.

Chapter 5 **: Conclusion & Summary**

6.1 Conclusion

This thesis focuses on the design of an over-coupled coaxial resonator that can be used to test and measure the electrical properties of materials. The concept behind the proposed methodology is based on the reflected group delay information.

Aside from the measurement of electrical properties of materials, the concepts used in this study provide an insight into the design of a lossy filter. The coupling capacitance for a coupled resonator can be obtained from the group delay information using the methodology developed, and when a dielectric sample is introduced into the resonator with same coupling maintained, the relative dielectric permittivity and loss tangent of the material can be determined. These quantities are the electrical properties of the dielectric sample material introduced into the resonator. Accurate information of the electrical properties of materials is useful when these materials are deployed in designs or other engineering purposes. For example, knowledge of dielectric constant of Teflon is necessary when it is used in transmission lines.

The results from the simulations using electromagnetic simulation software (HFSS) and measurements from the fabricated resonator were similar, and within acceptable percentage difference and limits when known values of dielectric samples were measured for both the simulation and the fabricated resonator.

This method of determining electrical properties of materials explores the accuracy of the resonant techniques of determining electrical properties and provide a convenient way of testing sample materials. The complexity associated with the perturbation method, for example, where it is required to accurately estimate a small quantity of material sample to

be tested with respect to the resonator that will give the desired perturbation and placing the sample at positions of maximum electric fields are eliminated. Also, solids that can be machined into the resonator diameter, powders and liquids of reasonable viscosity can be easily measured using the fabricated resonator. This provides a wide range of materials to be tested using this method. This method is also suitable for low-loss materials.

Most resonant techniques generally allow for measurements at single frequencies only; the resonant frequency, therefore broadband measurements cannot be done. However, the ability to vary the coupling capacitance obtained from tuning the inner conductor length of the resonator allows for measurements to be carried out over few megahertz (MHz). This is dependent on the range of coupling capacitance that will keep the resonator over-coupled. As such this method can allow for narrow band measurement of electrical properties. Also, with design parameters, the fabricated resonator can only measure and test different dielectric materials that will keep the resonator over-coupled. To measure those materials with higher dielectric and loss tangent values, the design parameters will be changed. This can be done by using coupled coaxial resonators of higher conductors' diameter and other factors that will increase the coupling capacitance.

6.2 Future Work

The motivation for this study was initiated with the need to investigate the electrical properties of soil. Further work is needed to adapt the concepts developed in this study to the determination of electrical properties of soil. Also, the use of inductive coupling to the resonator should be investigated. It was observed that the accuracy of the dielectric values reduces as the dielectric values increases. This could be a result of the resultant increase in coupling capacitance caused by the fringe capacitances from the end of the dielectric

material close to the gap spacing. Using inductive coupling, the fringe capacitances from the electric field applied to the dielectric material will be neglected in the value of the coupling values.

Also further work should be done to improve the fabrication process. With appropriate seal between the inner and outer conductor of the coaxial resonator, the fabricated resonator can be used in measuring liquids with less viscosity. The fabricated resonator should be properly calibrated to minimise errors from measurement.

Appendices

1. Solving for the coupling Capacitance using equation 3.7

```
Freq =327.70e6;% Resonator Frequency
DiameterRatio = 9.16290731E-01;% Ratio of the outer and inner Diamter of the resonator
GroupDelay=2.34629969e-8; % Group dealy Value at resonant frequency
InputReflection=0.9696674; %S11 @ Resonant Frequency
L= 0.18861; % Lenght of the resonator
Permittivity =1; %Since Empty Permittivity equals 1
B= (60*DiameterRatio * L)/3e8;
CouplingCoefficient = (1 + InputReflection)/(1-InputReflection);
LoadedQualityFactor = (2* InputReflection * 2* 3.141592653589793* Freq *GroupDelay)/(4*(InputReflection +1));
UnloadedQuality = (1 + CouplingCoefficient)*LoadedQualityFactor; %Unloaded Quality factor
Acoefficient = ((2*3.141592653589793*Freq)/(2*UnloadedQuality))^2;
Bcoefficient = (2*50)/GroupDelay;
a = Acoefficient; b= Bcoefficient; c=-2500;
syms x; %declare the variable x
y = a*x^2 + b*x  + c; %this leads to the quadratic  formula
dis = sqrt(b^2 - 4*a*c); %this is the discriminant
x1 = (-b + dis)/ (2*a)
x2 = (-b - dis)/ (2*a)
Qu = UnloadedQuality;
A1=-(x1-B);
B1=1/(2*3.141592653589793*Freq);
C1=(L*Permittivity)/(3e8*60*DiameterRatio);
syms U; %declare the variable x
y1 = A1*U^2 + B1*U  + C1; %this leads to the quadratic  formula
dis = sqrt(B1^2 - 4*A1*C1); %this is the discriminant
ReactiveCapacitance1 = (-B1 + dis)/ (2*A1); % a solution that satisfy the equation - Discared
ReactiveCapacitance2 = (-B1 - dis)/ (2*A1); % One of the solution of the equation Needed
CouplingCapacitance = ReactiveCapacitance2/(2*3.141592654*Freq) % COupling capacitance
```

1. Solving for the permittivity & loss tangent using equation 3.7 and equation 3.12

```
Freq =257.6e6; % Resonator Frequency
DiameterRatio =9.162907E-01; % Ratio of the outer and inner Diamter of the resonator
GroupDelay=6.895207e-8; % Group dealy Value at resonant frequency
InputReflection=0.9290693; %S11 @ Resonant Frequency
L=  0.18861; % Lenght of the resonator
ReactiveCapacitance2=(2*3.141592653589793*Freq*2.411742089085911e-12);% Reactive Reactance
B= (60*DiameterRatio * L)/3e8;
CouplingCoefficient = (1 + InputReflection)/(1-InputReflection); %Coupling COeffiecient K
LoadedQualityFactor = (2* InputReflection * 2* 3.141592653589793* Freq *GroupDelay)/(4*(InputReflection +1))% Loaded Quality Factor
UnloadedQuality = (1 + CouplingCoefficient)*LoadedQualityFactor; % Unloaded Quality Factor
Acoefficient = ((2*3.141592653589793*Freq)/(2*UnloadedQuality))^2;
Bcoefficient = (2*50)/GroupDelay;
a = Acoefficient; b= Bcoefficient; c=-2500;
syms x; %declare the variable x
y = a*x^2 + b*x  + c; %this leads to the quadratic  formula
dis = sqrt(b^2 - 4*a*c); %this is the discriminant
x1 = (-b + dis)/ (2*a)
x2 = (-b - dis)/ (2*a);
Qu = UnloadedQuality
B1=1/(2*3.141592653589793*Freq*ReactiveCapacitance2);
P=(x1-B-B1);
Permittivity=(P*3e8*60*DiameterRatio*ReactiveCapacitance2^2)/L% Extract relative permittivity
Qc = (2 * sqrt(3.141592653589793 *Freq * 58000000)* DiameterRatio)/0.22047244 % Quality factor due to the resonator
Losstangent = (1/Qu)-(1/Qc) % Extracting the loss tangent
```

2. Assembled fabricated device

3. Dismantled Resonator

4. Inside the coupling Section

5. Samples of Teflon

References

Amphenol RF. (2017, July 5). Retrieved from Amphenol: http://www.amphenolrf.com/082-6330.html

App. Note, A. (2006). *Agilent Basics of Measuring the Dielectric Properties of Materials.* Agilent Literature Number.

Arulanandan, K. (2003). *Soil structure: in situ properties and behavior.* University of California, Davis: Department of Civil and Environmental Engineering.

Baker-Jarvis, J. V. (1990). Improved technique for determining complex permittivity with the transmission/reflection method., . *IEEE Transactions on microwave theory and techniques, 38(8)*, 1096-1103.

Cameron, R. J. (2007). *Microwave filters for communication systems.* Wiley-Interscience.

Chua, L. H.-S. (2003). Accurate and direct characterization of high-Q microwave resonators using one-port measurement. *IEEE transactions on microwave theory and techniques, 51(3)*, 978-985.

Drozd, J. M. (1996). Determining Q using S parameter data. *IEEE transactions on microwave theory and techniques*, , 44(11), 2123-2127.

Ehrlich, P. L. (1953). Dielectric properties of teflon from room temperature to 314 C and from frequencies of 102 to 105 c/s. *Conference on Electrical Insulation*, (pp. 28-30).

Ghodgaonkar, e. a. (1989). A free-space method for measurement of dielectric constants and loss tangents at microwave frequencies. *IEEE Transactions on Instrumentation and measurement, 38(3)*, 789-793.

Guo, W. Y. (2013). Frequency, moisture, temperature, and density-dependent dielectric properties of wheat straw. . *Transactions of the ASABE, 56(3)*, 1069-1075.

Hengcharoen, T. K. (2011). Microwave dielectric measurement of liquids by using waveguide plunger technique. *Procedia Engineering 8*, 270-274.

Jha, S. N. (2011). Measurement techniques and application of electrical properties for nondestructive quality evaluation of foods—a review. *Journal of food science and technology* , 387- 411.

Kaatze, U. (2010). Techniques for measuring the microwave dielectric properties of materials. . *Metrologia, 47(2)*, S91.

Kraszewski, A. W. (1992). Observations on resonant cavity perturbation by dielectric objects. . *Microwave Theory and Techniques IEEE Transactions on 40(1)*, 151-155.

Laforge, P. D., Mansour, R., & Yu, M. (2010). The design of miniaturized superconducting filters with the reflected group delay method. *IEEE Transactions on Applied Superconductivity, 20(4),*, 2265-2271.

Li, D. F. (2001). "A simple method for accurate loss tangent measurement of dielectrics using a microwave resonant cavity. *IEEE microwave and wireless components letters*, 118-120.

Liu, N. ((2007). *Soil and site characterization using electromagnetic waves .* Virginia Tech: Doctoral dissertation.

Microwave101. (2017, July 25). Retrieved from Mcrowave101: https://www.microwaves101.com/encyclopedias/miscellaneous-dielectric-constants

Nelson, S. O. (2010). Fundamentals of dielectric properties measurements and agricultural applications. *Journal of Microwave power and electromagnetic energy, 44(2),* , 98-113.

Ness, J. B. (1998). A unified approach to the design, measurement, and tuning of coupled-resonator filters. *IEEE Transactions on Microwave Theory and Techniques, 46(4)*, 343-351.

Palanikumar, M. (2013). *Soil Mechanics.* PHI Learning Pvt. Ltd.

Pozar, D. M. (2009). *Microwave engineering.* John Wiley & Sons.

Robinson, J. B.-H. (2014). Microwave processing of oil sands and contribution of clay minerals. *Fuel*, 135, 153-161.

Santos, J. C. (2009). *Using the coaxial probe method for permittivity measurements of liquids at high temperatures.* Journal of Microwaves, Optoelectronics and Electromagnetic Applications (JMOe).

Sharma, S. K. (2013). Cavity perturbation measurement of complex permittivity of dielctric material at microwave frequencies. *International Journal of Emerging Technologies in Computational and Applied Sciences (IJETCAS)*, 116-120.

Sheen, J. (2005). Study of microwave dielectric properties measurements by various resonance techniques. *Measurement Science and Technology*, 37(2), 123-130.

Smyth, C. P. (1955). *Dielectric behavior and structure.* New York: McGraw-Hill Book Co., Inc.

Trabelsi, S. N. (2003). Free-space measurement of dielectric properties of cereal grain and oilseed at microwave frequencies. *Trabelsi, S., & Nelson, S. O. (2003). Free-space measurement of dielectric properties of cereal grain and oilseed at microwave frequencies. Measurement Science and Technology, 14(5), 589.*, 589.

Wu, M. X. (2000). "An improved coaxial probe technique for measuring microwave permittivity of thin dielectric materials. *Measurement science and technology*, 1617.

Wu, M. Y. (2000). An improved coaxial probe technique for measuring microwave permittivity of thin dielectric materials. *Measurement science and technology*, 11(11), 1617.

Yen, B. C. (2013). Advances in Hydroscience. *Elsevier*, Vol. 14.